UNIVERSITY OF INSUBRIA

DOCTORAL SCHOOL IN BIOLOGICAL AND MEDICAL SCIENCES

PHD PROGRAM IN NEUROBIOLOGY


# PHENOTYPIC AND MOLECULAR CONSEQUENCES OF A PATHOGENIC MISSENSE MUTATION IN *MECP2*: CHARACTERIZATION OF A NOVEL MOUSE MODEL

Relatore: Prof.ssa Nicoletta Landsberger
Coordinatore: Prof.ssa Daniela Parolaro

Tesi di Dottorato di:
Anna Gandaglia
Matr N. 720560

Anno Accademico 2014/2015
Ciclo XXVIII

# Abstract

Rett syndrome (RTT) is a devastating genetic disease that affects predominantly girls. It is characterized by a host of neurological symptoms of variable severity and it is primarily caused by sporadic mutations in the X-linked Methyl-CpG binding protein 2 (*MECP2*) gene. Over the years, different mouse models mutated in *Mecp2* – well recapitulating the human disorder – have been instrumental for understanding some aspects of RTT pathogenesis and of MeCP2 biological activities. This protein appears as a multifunctional molecule involved in many different processes, such as transcriptional regulation and chromatin compaction. However, several aspects regarding MeCP2 and the consequences of its alterations need further deeper investigation. In particular, new interest is rising on the post-translational modifications found along the protein, which are hypothesized to regulate its multiple biological functions. In this context, the Tyr-120 residue of MeCP2 appears worth of interest since it is both subjected to phosphorylation and associated with the development of Rett syndrome, with its substitution to aspartic acid resulting pathogenic in humans. Previous *in vitro* studies aimed at characterizing the Tyr-120 phospho-isoform permitted to reveal a novel localization of the protein at the centrosome and a functional association with this cellular organelle. To better investigate the relevance of this amino acid site and of its defective phosphorylation we generated a knock-in mouse model carrying the disease-causing Y120D mutation. Here we present the phenotypic, morphological and molecular characterization of this novel mouse line. We show that C57BL6J and CD1 *Mecp2*$^{Y120D}$ mice suffer from a host of RTT-like phenotypes, while the mutated neuronal cells and tissues do not present some of the abnormalities typically found in *Mecp2*-null models. Importantly, the Y120D alteration causes the subnuclear delocalization of the protein from pericentromeric heterochromatic foci. Moreover, adult, but not immature, brains from knock-in animals are characterized by altered levels of Mecp2 and of one of its phospho-isoforms. They also show increased solubility of the mutated protein and reduced chromatin compaction. Overall, these molecular defects – together with other aspects that need to be better analysed – likely contribute to the pathogenic mechanisms leading to RTT-like phenotypes. We believe that the study of this new genetically engineered mouse model will help to shed light on the importance of MeCP2 post-translational modifications and on their relevance in RTT pathogenesis.

# INDEX

# 1. Introduction

Rett syndrome (RTT, OMIM # 312750) is a severe and progressive neurological disorder that affects almost exclusively females with an incidence of ≈ 1/10000 live births, representing therefore one of the main causes of severe intellectual disability worldwide (Percy and Lane, 2005). The high majority of RTT cases is sporadic; however, through the study of rare familial examples of this genetic disease, in 1999 mutations in the X-linked Methyl-CpG binding Protein 2 (*MECP2*) gene were identified as the primary molecular cause of Rett syndrome (Amir et al., 1999). Since then, great efforts have been made by the scientific community to reach a deep comprehension of RTT pathogenesis and MeCP2 functions, with the ultimate aim of finding an effective treatment for this devastating disorder.

## 1.1. Rett syndrome: from clinical manifestations to mouse models

### *1.1.1. Clinical course of classic RTT*

Firstly reported in 1966 by Dr. Andreas Rett and better described in 1983 by the neurologist Bengt Hagberg (Hagberg et al., 1983), classic RTT patients present a typical clinical course that can be divided into four distinct phases (Figure 1). At around 6-18 months of life, after a period of apparent normal development in which girls achieve the milestones proper of their age (such as the ability to walk), Rett syndrome starts to manifest and seemingly healthy-look babies fall into the first phase of the disease: the developmental stagnation. At this time, patients show deceleration in head growth that leads to acquired microcephaly, overall growth retardation, weight loss, muscle hypotonia and weak posture. Language development remains poor and the interactive behaviour of girls starts to change, with some of them becoming for example irritable and restless. Then, between 1 and 4 years of age, RTT girls experience a rapid regression phase that affects cognitive, communication and motor skills and that is considered a hallmark of the disease. Patients loose the previously acquired abilities, such as walking and word use or babbling. Purposeful hand use is replaced by continuous stereotypic movements of small magnitude, as hand wringing, washing or clapping. Girls develop autistic features: they manifest indifference to the surrounding environment, social withdrawal and also self-abusive behaviour. Moreover, motor dysfunctions such as apraxia and gait ataxia are developed. Seizures of variable severity and respiratory abnormalities often begin to manifest

during this stage. In the following pseudo-stationary phase, which can last for decades, the autistic-like behaviour somehow ameliorates. Seizures can still be present and breathing anomalies may become more severe. At this time, RTT girls suffer from scoliosis, rigidity, dystonia, autonomic dysfunctions and anxiety episodes. Motor dysfunctions continuously progress, causing most RTT patients to become wheelchair-dependent at the beginning of the late motor deterioration phase, in which girls present pronounced muscle wasting and frozen rigidity or Parkinsonian features. This debilitating situation then reaches a plateau and some affected individuals survive until sixty or seventy years of age (Chahrour and Zoghbi, 2007; Lombardi et al., 2015; Smeets et al., 2012).

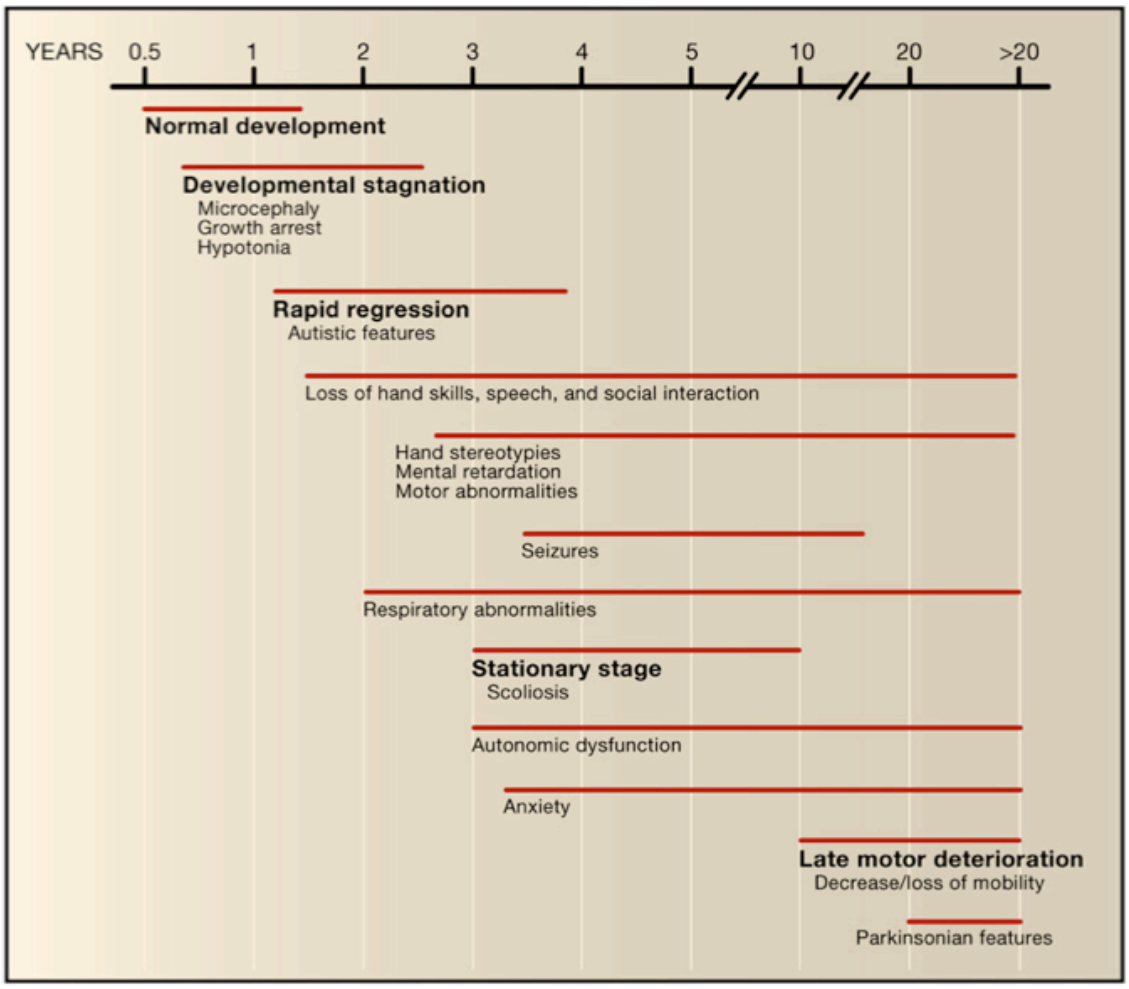


**Figure 1. The cascade of clinical symptoms in classic Rett syndrome** (Chahrour and Zoghbi, 2007)**.**

It is now well recognized that the severity and progression of the described symptoms vary greatly between the different affected individuals; accordingly, several variant or atypical forms of RTT, ranging from milder to more severe clinical pictures, are currently diagnosed. While *MECP2* mutations are found in more than 95% of classical cases, they are reported in

50 to 70% of the atypical ones and other genes – such as *FOXG1* and *CDKL5* – have been associated to them (Ariani et al., 2008; Chahrour and Zoghbi, 2007; Kilstrup-Nielsen et al., 2012; Neul et al., 2010). Hemizygous males with loss-of-function *MECP2* alterations that lead to RTT in girls generally die early after birth because of severe neonatal encephalopathy. However, male RTT cases have been identified mainly in individual with X-chromosome aneuploidy or somatic mosaicism; milder mutations, leading to subtle clinical manifestations in females, can also cause RTT in boys. Moreover, genetic screenings have demonstrated that deviations in *MECP2* can result in a broad spectrum of disorders, including autism, Angelman-like syndrome, female microcephaly and severe to mild intellectual disabilities (Chahrour and Zoghbi, 2007; Erlandson and Hagberg, 2005). Genotype-phenotype correlation studies have highlighted that several factors can contribute to the described phenotypic variability such as the type and position of the gene mutation and the pattern of X chromosome inactivation (XCI), that represents a major source of this variability. Although the choice of which X chromosome has to be inactivated is usually random, skewed X inactivation – favouring the expression of the wild-type allele – has been observed in several patients. The extent of amelioration of RTT phenotypes depends on the degree of favourable skewing: some women can even be asymptomatic carriers of *MECP2* alterations, and, thus, can transmit the mutant allele to their offspring, giving rise to rare familial cases. Eventually, somatic mosaicism and still unrecognized modifier genes may influence the clinical outcome of the disease (Chahrour and Zoghbi, 2007; Schanen et al., 2004).

### *1.1.2. Rett syndrome mouse models recapitulate human phenotypes*

Along the last 15 years several mouse models of *Mecp2* alterations have been generated; overall, they have provided the definitive evidence of the association between RTT and *MECP2* and have been fundamental for the current comprehension of the pathogenesis of the disorder. Indeed, mice carrying different gene mutations phenotypically well recapitulate the human disease (Ricceri et al., 2008).

Since Rett syndrome predominantly affects girls, the most appropriate genetic mouse model of this disease is the heterozygous female. However, the majority of works in the field has focused on hemizygous male mice, which usually develop a worse condition. The primary reasons for this discrepancy reside in the longer time required for symptoms appearance in mutated female mice and in their phenotypic variability, deriving from the X-chromosome

inactivation phenomenon, which could have confounding effects. Consequently, at the moment, male mice are considered a suitable model to investigate the role of the protein on the development of RTT-like phenotypes (Ricceri et al., 2008).

The first two RTT mouse models were generated in 2001 and probably still represent the two mostly used and characterized ones (Chen et al., 2001; Guy et al., 2001). The mutated *Mecp2* allele obtained by Guy et al. lacks exons 3 and 4, while the one from Chen et al. lacks only exon 3. Both deletions block *Mecp2* expression in the entire organism, therefore the hemizygous male mice (*Mecp2*$^{-/y}$) represent *Mecp2*-null models. Similarly to patients, *Mecp2*$^{-/y}$ mice present an early apparent normal developmental phase that lasts for 3-6 weeks of age; then, they undergo a rapid regression in which gross abnormalities start to manifest and rapidly worsen, leading to premature death at around 8-10 weeks of age. These mice suffer from severe neurological impairments, reduced spontaneous movements, stiff uncoordinated gait, hypotonia, hind limb clasping, irregular breathing, tremors and often seizures. C57BL6J *Mecp2*-null males also show reduced body weight; however, this feature seems to depend on the genetic background, as recently confirmed by a study carried out in our laboratory (Cobolli Gigli et al., *paper under revision*). Testes are always internal in the mice described by Guy et al. (known as *Mecp2*$^{Bird}$), which therefore are infertile (Chahrour and Zoghbi, 2007; Conti et al., 2015; Ricceri et al., 2008).

Heterozygous females (*Mecp2*$^{+/-}$) are fertile and appear normal for the first 3-4 months of age, when they start to slowly develop RTT phenotypes, such as hypoactivity, hind limb clasping, uncoordinated gait and, later, breathing abnormalities. In contrast with male mice, females have been reported to become overweight (again depending on the genetic background) and usually survive for more than 10 months of age (Lombardi et al., 2015; Ricceri et al., 2008; Samaco et al., 2013). Notably, being the *Mecp2*-null males infertile, heterozygous females are precious and necessary to maintain the mouse lines.

Similarly to patients, these RTT mouse models display reduced brain size and weight, without any obvious sign of neurodegeneration or neuroinflammation and without gross neuropathological changes. Reminding again what is found in girls affected by Rett syndrome, *Mecp2*-null neurons show anomalies in axon orientation, smaller somas, altered spines and reduction in dendritic branching, abnormalities in neurotransmitter concentrations and impairments in synaptic functions (Armstrong, 2005; Belichenko et al., 1994; Belichenko et al., 2009; Chahrour and Zoghbi, 2007; Conti et al., 2015; Lombardi et al., 2015).

From 2001 onwards, many other models with less severe genetic lesions, often similar to RTT-causative mutations in humans, have been generated. For example, the *Mecp2*$^{308X}$ mouse (Shahbazian et al., 2002a), mimicking the late truncating mutations commonly found in classic RTT, is characterized by a hypomorphic gene alteration that has milder consequences with respect to the null allele, although still recapitulating many features of Rett syndrome. In fact, after a period of apparent normality lasting almost the first 6 weeks of age, *Mecp2*$^{308/y}$ mice progressively develop hypoactivity and motor impairments, stereotypies, kyphosis, tremors, seizures and anxious behaviour (Shahbazian et al., 2002a).

| | | Null mice | | *Mecp2*$^{308X}$ |
|---|---|---|---|---|
| | **Rett** | **Males** | **Het females** | **Males** |
| Motor | Limited mobility | + | + | + |
| | Ataxic gait | + | + | + |
| | Dystonia/rigidity | + | + | + |
| | Tremor | + | + | + |
| | Stereotypies | – | – | + |
| Cognitive and social abilities | Decreased cognition | + | + | + |
| | Speech loss | ND | ND | ND |
| | Social avoidance | – | + | – |
| | Anxiety | * | * | + |
| Morphological | Microcephaly | + | – | – |
| | Neuronal hypotrophy | + | + | – |
| Autonomic dysfunction | Breathing abnormalities | + | + | ND |
| | Reduced lifespan | + | + | + |
| Other | Seizures | + | – | + |

**Table 1. Face validity of *Mecp2* loss-of-function mouse models** (adapted from (Lombardi et al., 2015))**.**

Altogether, the similarities between pathological phenotypes in RTT girls and in RTT mice (Table 1) underlie the face validity of MeCP2 loss-of-function mouse models, which are, therefore, instrumental for the study of the pathogenic mechanisms of the disease and suitable for the development and testing of possible therapeutic approaches.

From the employment of mice, in 2007 came the major breakthrough in the field of Rett syndrome that is the reversibility of the neurological phenotypes in MeCP2 disorders, even at late stages of the disease. In fact, Dr. Bird and colleagues (Guy et al., 2007) demonstrated that reactivation of the endogenous *Mecp2* gene results in reversal of several RTT symptoms and in normal lifespan in both young and adult symptomatic *Mecp2*$^{-/y}$ and *Mecp2*$^{+/-}$ animals. These data, supported by other related studies, indicate that MeCP2 deficiency does not permanently damage neurons – a finding that is consistent with the lack of neurodegeneration in RTT brains – and prompted the scientists to search for valid therapeutic strategies aimed –

for example – at obtaining the restoration of the protein endogenous levels in mouse models and patients (Giacometti et al., 2007; Guy et al., 2007; Luikenhuis et al., 2004).

## 1.2. MeCP2: what is known and what is still missing about this multifunctional protein

### *1.2.1. MeCP2 binding and structural properties*

Before a causative connection between *MECP2* alterations and Rett syndrome was established, the MeCP2 protein had already been described by Dr. Bird and colleagues as a nuclear factor binding *in vitro* to DNA containing at least one symmetrically methylated CpG-dinucleotide and accumulating in mouse cells on highly methylated pericentromeric heterochromatin (Lewis et al., 1992).

*MECP2* maps in Xq28 and consists of four exons that code for a ubiquitously expressed protein vastly conserved among mammals, which contains a methyl-CpG binding domain (MBD), therefore, belonging to the methyl-CpG binding protein family of transcriptional regulators (Lewis et al., 1992; Samaco and Neul, 2011).

Since different polyadenylation signals are present, the *MECP2* transcript can go from 1.8 to 10 kilobases: the last one is the predominant form in brain and is characterized by a highly conserved 8.5-kb-long 3'UTR (Pelka et al., 2005; Samaco and Neul, 2011). Because of alternative splicing of exons 1 and 2, two isoforms of the protein exist (Figure 2): MeCP2e1 is 498 residues long, while MeCP2e2 is made of 486 amino acids. The two isoforms differ only in their N-terminal residues and for their expression profiles. Indeed, the long one is 10-fold more abundant in mouse brains than the short one, which conversely is more expressed in placenta and liver. However, since pathogenic mutations of

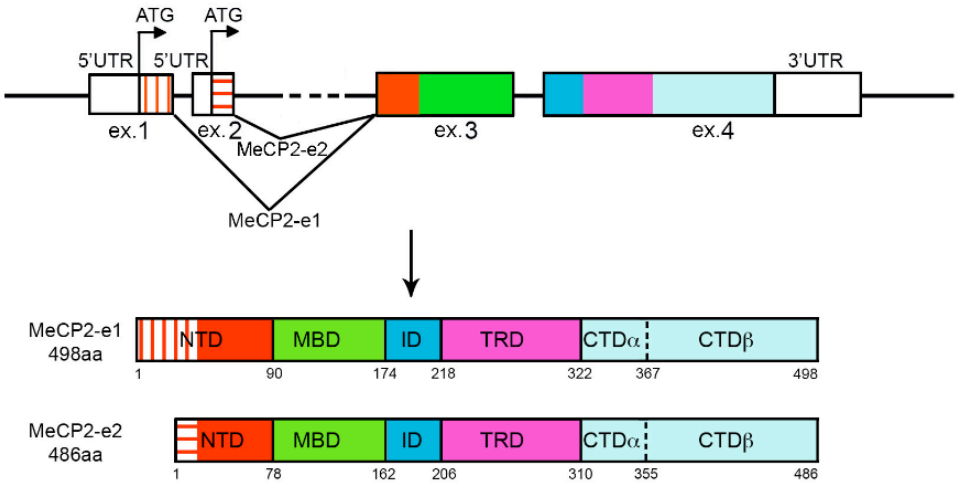


**Figure 2. MeCP2 splicing isoforms and domains** (Bedogni et al., 2014).

*MECP2* generally occur in exons 3 and 4, these two isoforms are considered mainly functionally equivalent (Bedogni et al., 2014; Itoh et al., 2012; Kriaucionis and Bird, 2004).
In addition to the MBD, that in MeCP2e2 spans from residue 79 to 162, MeCP2 contains other 4 distinct domains (Figure 2): the N-terminal domain (NTD, from residue 1 to 78), the intervening domain (ID, residues 163-206), the transcriptional repression domain (TRD, residues 207-310) and the C-terminal domain (CTD, that can be further subdivided in CTDα and CTDβ, respectively from residue 311 to 355 and from residue 356 to 486) (Figure 2) (Bedogni et al., 2014).
The MBD was the first domain to be functionally defined and – so far – the only one whose structure has been solved by NMR and crystallography. Its relevance is highlighted by the fact that almost 40% of RTT-causing missense mutations (with frequency higher than 0.1%) occurs in this portion of the protein (Bedogni et al., 2014). Even if more than 20 years have passed since the first description of MeCP2 as a methyl-CpG binding factor, the full properties of its MBD are still far from being completely understood. Recently, it has been demonstrated that the MBD is structurally and/or functionally coupled with the NTD, the ID and the TRD. In particular, the conformational coupling between the NTD and the MBD appears to synergistically increase the binding affinity for methylated DNA (Ghosh et al., 2010b). Interestingly, a recent study identified MeCP2 as the major 5-hydroxymethylcytosine (5hmC)-binding protein in brain. 5hmC is a novel epigenetic signal whose functions are still under investigation; however, it seems to be mainly present in neuronal cells, where it is enriched in active genes. Of relevance, the disease-causing R133C mutation – usually found in patients with milder form of Rett syndrome – preferentially inhibits the binding of MeCP2 to 5hmC, while preserving most of the 5mC binding affinity. In the future, it might be important to associate MeCP2 specific binding to 5hmC with specific molecular pathways altered in RTT (Mellen et al., 2012). Finally, very recently it has been demonstrated that the MBD of MeCP2 can also bind methylated cytosines not belonging to a CpG dinucleotide (mCH; H=A, C, T), another epigenetic signal particularly abundant in adult brain (Chen et al., 2015; Lombardi et al., 2015). *It is conceivable that each of these marks could be associated with a different functional feature of MeCP2 and, therefore, a deep characterization of these associations could be significant for a full comprehension of MeCP2 activities.*

Eventually, *in vitro* MeCP2 is also capable of binding unmethylated DNA through non-specific binding sites contained in the ID, TRD and CTDα domains (Figure 3). Whether this capability is retained *in vivo* is highly debated. Indeed, it has been shown that in neurons,

where MeCP2 is extremely abundant and genome-wide bound, the protein specifically tracks methyl-CpG density. A possible explanation for this apparent contradiction between *in vitro* and *in vivo* data is that a weak binding of the full-length protein to unmethylated DNA could facilitate the subsequent association of the MBD with the methylated sequences and, on the other hand, induce structural/functional changes of the different domains (Bedogni et al., 2014; Ghosh et al., 2010b; Skene et al., 2010).

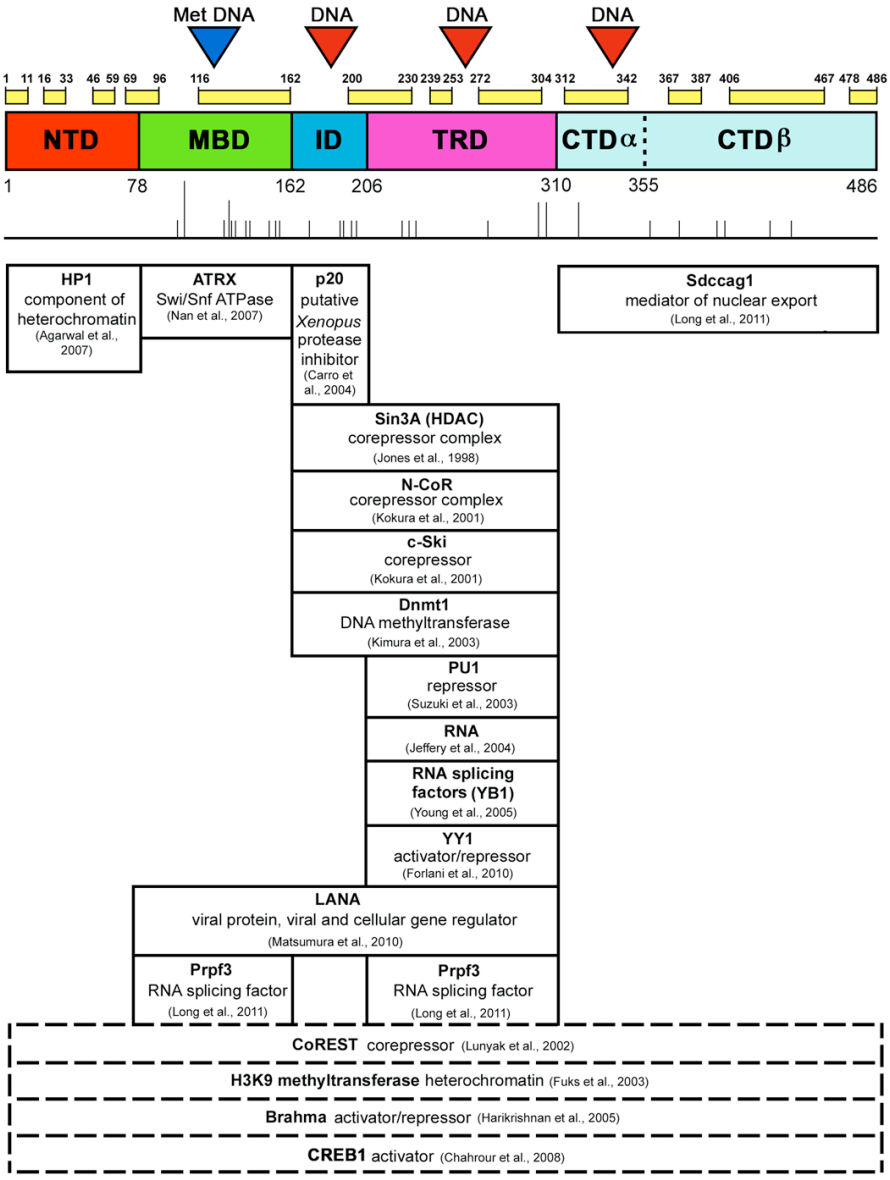


**Figure 3. Binding properties and structural features of MeCP2.** Blue and red triangles indicate binding to methylated and unmethylated DNA respectively. The yellow bars represent predicted disordered binding regions. Vertical lines indicate missense mutations with a frequency higher than 0.1%. Boxes highlight the interacting partners of MeCP2, relative to the involved MeCP2 regions. Dashed boxes indicate still unmapped interactions (adapted from (Bedogni et al., 2014)).

The second domain of MeCP2 to be functionally identified was the transcriptional repression domain (TRD). Most of its activity is exerted through the recruitment of additional molecules, such as the corepressor complexes Sin3A and N-CoR that contain histone deacetylase activities, therefore leading to chromatin compaction. Other interacting partners of the TRD are the corepressor c-Ski, the DNA methyltransferase Dnmt1 and the transcription factor YY1 (Figure 3) (Bedogni et al., 2014).
Although the CTD molecular functions remain largely uncharacterized, *in vitro* it is required for chromatin interactions (Ghosh et al., 2010b).
Importantly, RTT-causing missense and nonsense mutations occur throughout the entire coding sequence of MeCP2, highlighting the relevance of all domains for the protein functions (Hansen et al., 2010).

Apart from the MBD and the TRD domains, which have been identified because of their main activity, information on the described organization in six domains were obtained through limited protease digestion. Indeed, digestion of MeCP2 with trypsin reproducibly gives rise to a pattern of six peptides corresponding to the described portions of the protein (Adams et al., 2007; Hansen et al., 2010). Since almost 60% of the full-length protein is unstructured in solution, structural data exist only for the methyl-binding domain; in other words, MeCP2 is an intrinsically disordered protein (Adams et al., 2007). This is a relatively new concept that can represent the molecular basis of protein multifunctionality; indeed, disorganized proteins acquire local secondary structure upon binding to partners. Accordingly, bioinformatic software predict that MeCP2 harbors an unusually large number of MoRFs (molecular recognition features) and disordered binding regions that undergo a disorder-to-order transition, acquiring folded secondary structure, after binding (Figure 3) (Bedogni et al., 2014; Ghosh et al., 2010b). Thus, MeCP2 can be considered as a recruitment platform for different partners, justifying – at least in part – its multifunctionality. Indeed, beside the already listed partners, MeCP2 appears to interact with several other factors, such as the component of heterochromatin HP1, the Swi/Snf proteins ATRX and Brahma, RNA and RNA splicing factors, the methyltransferase H3K9, the corepressor CoREST and the transcriptional activator CREB (Figure 3 and listed references).

### *1.2.2. MeCP2 functions and RTT pathogenic mechanisms*

Despite the intense research activities carried out in the last decades, many questions about MeCP2 functions are still open.

As mentioned, MeCP2 is usually regarded as a transcriptional repressor, due to its ability to bind an epigenetic repressive mark and to inhibit transcription both of reporter gene *in vitro* and in natural settings (Figure 4). Because of this view, several transcriptional profiling studies have been performed on brains from *Mecp2*-null mice or on human post-mortem brains in order to identify the target genes of the protein. However, this approach failed to reveal consistent expression changes and, at the moment, there are only few genes recognized as *bona fide* targets of MeCP2 (Chahrour and Zoghbi, 2007). These results led to hypothesize that – at least in brain – MeCP2 does not control the expression of single genes and/or that its loss causes only modest variations in transcription (Guy et al., 2011).

New hints on MeCP2 roles in brain were given in 2010 when it was demonstrated that in neuronal nuclei MeCP2 is almost as abundant as nucleosomes and methyl-CpG moieties (1.6 x $10^7$ molecules *versus* 3 x $10^7$ and 5 x $10^7$ molecules respectively) and, therefore, it is distributed throughout the genome (Skene et al., 2010). This extreme abundance together with previous *in vitro* studies demonstrating that MeCP2 binds the linker DNA competing with the H1 histone (Ghosh et al., 2010a) and that, at a high molar ratio to nucleosomes, MeCP2 mediates the formation of a novel highly compacted chromatin structure (Georgel et al., 2003), led the authors to hypothesize that in mature neurons MeCP2 acts as a histone-like constitutive component of the chromatin, globally modulating its structure and dampening transcriptional noise. Consistently with this view, in *Mecp2*-null neurons histone acetylation levels are enhanced, histone H1 concentration is doubled and there is a general derepression of repetitive elements (Bedogni et al., 2014; Muotri et al., 2010; Skene et al., 2010).

This model, however, leaves unanswered an important question: which is the mechanism of action of MeCP2 in non-neuronal cells, where the protein is far less expressed? We speculated that MeCP2 is an architectural chromatin molecule that turns into gene specific transcription factor according to its abundance (Bedogni et al., 2014).

Furthermore, transcriptome analyses of murine hypothalamus and cerebellum showed that many genes are slightly downregulated in the absence of Mecp2 and upregulated when the protein is overexpressed, indicating that MeCP2 may also activate gene transcription, for example through the interaction with CREB1 (Chahrour et al., 2008). Given the enrichment of 5hmC in active genes, it should be interesting to study if the ones found downregulated in the lack of MeCP2 are also marked by this epigenetic signature.

The identification of the MeCP2 interaction with the alternative splicing factor YB1 and the spliceosome component Prpf3 suggested that MeCP2 might also play a role in the regulation of mRNA splicing (Long et al., 2011; Young et al., 2005).

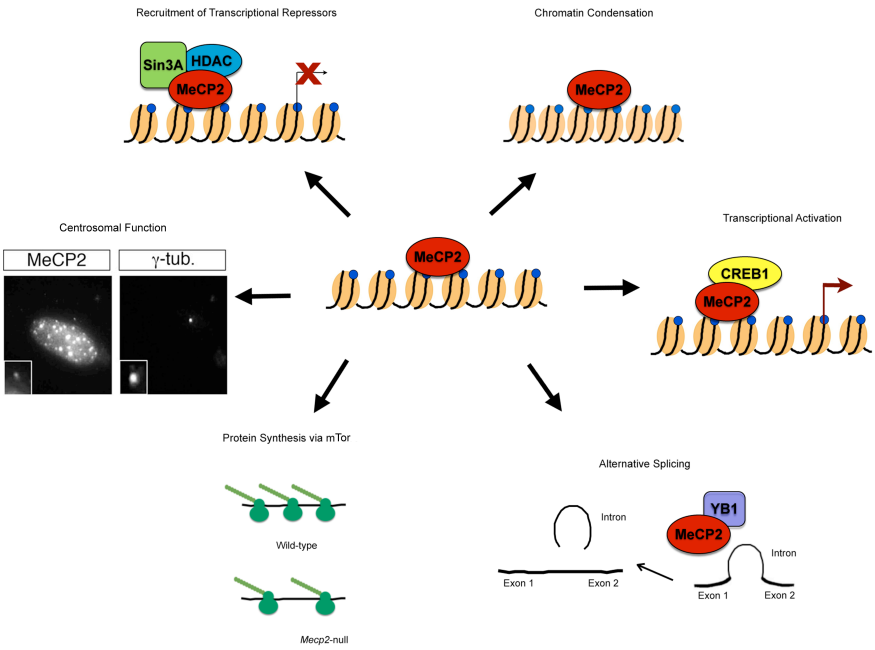


**Figure 4. Multifunctionality of MeCP2 (**adapted from (Bedogni et al., 2014))

MeCP2 is also involved in protein synthesis regulation through the IGF1 and the AKT/mTOR pathways (Ricciardi et al., 2011). The balance between protein synthesis and degradation is fundamental for the maturation and homeostasis of tissues and aberrant translation is often observed in autism-spectrum diseases (Kelleher and Bear, 2008). Accordingly, *Mecp2*-null mice show reduced plasma levels of the growth hormone IGF1. Reduced phosphorylation of the ribosomal protein S6 and impaired protein synthesis have been found in the brain of male and female mouse models before the appearance of RTT symptoms. However, whether MeCP2 directly interacts with the translational apparatus or whether the described defects are a secondary consequence of its deficiency still has to be determined (Conti et al., 2015; Ricciardi et al., 2011).

Eventually, a novel function of MeCP2 has been indicated by the unexpected observation of the protein localization at the centrosome both in proliferating and post-mitotic cells. Remarkably, Mecp2 deficient cells show altered microtubule nucleation and abnormal geometry of the mitotic spindle, affecting the duration of cell division that results prolonged.

These phenotypes, resembling those found in the absence of many centrosomal proteins, suggest that MeCP2 might be required for the proper function of this organelle and, thus, for cell cycle progression and proper neuronal maturation (Bergo et al., 2015).

A fundamental gap of knowledge in the Rett syndrome field is *when* and *where* the deficiency of the methyl-binding protein causes the cellular changes that lead to the RTT pathogenesis.
Concerning its expression in the central nervous system (CNS), the general acceptation was that the protein is mainly produced by mature neurons. However, a very recent study (Bedogni et al., 2015) has demonstrated that MeCP2 is expressed in a large set of neural cell types since the early stages of cortical development; indeed, low levels of MeCP2 are detected even in cortical neuroblasts at the embryonic day E10.5 and in progenitors and in both immature and mature neurons at E14.5. The protein abundance, however, depends on the stage of cellular maturation, greatly increasing during the postnatal development of the cortex, therefore suggesting an involvement of MeCP2 in neuronal maturation, maintenance and synaptogenesis (Kishi and Macklis, 2004). The relevance of the protein in these processes is confirmed by the morphological and neurophysiological changes observed in Mecp2 deficient neurons, which, as said before, show altered synaptic structure and function that influence neuronal networks activity. Importantly, the CamKII-Cre mediated deletion of *Mecp2* from forebrain post-mitotic neurons leads to a neuronal phenotype similar to the *Mecp2*-null manifestations (Chen et al., 2001) and the postnatal re-activation of *Mecp2* in mice rescues RTT-like symptoms (Guy et al., 2007). All in all these data indicate that MeCP2 plays a critical role in postnatal maintenance and synaptic plasticity of mature neurons, and have led the RTT field to question the importance of the protein in early brain development. Accordingly, it has recently been demonstrated that the deletion of *Mecp2* from fully adult mice (at 60 days of age) gives rise to phenotypes similar to those of germline *Mecp2*-null animals, underlying the requirement of the protein expression in adult life (McGraw et al., 2011).
However, recent data demonstrated that transcriptional alterations appear early during *Mecp2*-null embryonic cortical development, impacting neuronal maturation and appropriate responsiveness to stimuli. Therefore, MeCP2 seems to play an important role in regulating the transcriptional mechanisms proper of the developing embryonic neocortex. It is conceivable that the observed early defects worsen over time, likely contributing to the manifestation of postnatal symptoms, thus representing an important aspect of RTT pathogenesis (Bedogni et al., 2015).

Moving to the "where" part of the initial question, the predominant neurological phenotypes found in *MECP2*-disorders and the great abundance of the protein in neurons have clearly indicated the central nervous system as the major player in the clinical course of Rett syndrome. Whether other organs and cellular types contribute to the disease pathogenesis is still under discussion and conflicting data have been reported. Indeed, specific depletion of *Mecp2* from neurons (using the already described CamKII-Cre transgene) causes a RTT-like phenotype and *Tau*-driven specific expression of the protein in postmitotic neurons rescues the neurological symptoms of the null mice, strongly suggesting that RTT is almost exclusively caused by Mecp2 deficiency in neurons (Chen et al., 2001; Luikenhuis et al., 2004). However, MeCP2 is expressed in all types of glial cells and, thus, its absence might influence neuronal health in a non-cell autonomous fashion. Accordingly, co-culture of wild-type hippocampal neurons with *Mecp2*-null astrocytes leads to aberrant morphology of neurons that lack fine processes and have an increased number of short stunted dendrites, resembling what seen in RTT patients and suggesting that mutant astrocytes fail to support normal neuronal growth (Ballas et al., 2009). Moreover, specific re-activation of *Mecp2* in astrocytes of null mice significantly ameliorates RTT symptoms (Lioy et al., 2011). Altogether, these findings indicate the involvement of glial cells in Rett syndrome pathogenesis through different possible mechanisms that need to be better investigated and that could represent new therapeutic targets. The role of microglia in RTT has been recently highly debated. In fact, the group of Kipnis demonstrated that wild-type bone marrow transplantation into irradiated *Mecp2*-null mice arrests the progression of neurological symptoms and prolongs lifespan of the animals, through repopulation of brain parenchyma by wild-type microglial cells. Similar results were obtained expressing *Mecp2* specifically in myeloid cells – the lineage from which microglia derives – of otherwise null mice. The authors proposed that RTT neuronal dysfunction is partly caused by a decreased phagocytic capacity of *Mecp2* deficient microglia, probably causing debris accumulation in RTT brains; the protective effect of wild-type microglia would be exerted through the recovery of this phagocytic activity (Derecki et al., 2012). However, these data are now under discussion, since other groups didn't manage to obtain the same positive results after bone marrow transplantation (Wang et al., 2015). Nevertheless, new attention on the role of microglia and immune cells in Rett syndrome has recently arisen with the observation that MeCP2 is required for the proper inflammatory responsiveness of these cellular types. Indeed, in *Mecp2*-null mice, macrophages exhibit dysregulated transcriptional response to inflammatory

stimuli and are progressively depleted in various tissues, possibly contributing to the development of RTT symptoms (Cronk et al., 2015).

Notably, overexpression of *Mecp2* in mice resulted in fetal death caused by cardiac septum hypertrophy and in skeletal abnormalities, thus indicating a role for the methyl-binding protein in heart and skeleton development (Alvarez-Saavedra et al., 2010).

Given the necessity to better define the contribution of peripheral tissues to the pathogenesis of the disease and considering the severe hypotonia, muscle weakness and muscle wasting that affect girls with Rett syndrome and the animal models, we decided to investigate whether the lack of MeCP2 influences the health of the skeletal muscle and whether the protein plays a direct role in the homeostasis of this tissue [*see the attached paper* (Conti et al., 2015)]. Importantly, we demonstrated that in *Mecp2*-null mice skeletal muscles are characterized by a disorganized structure, with hypotrophic fibers and tendency to fibrotic tissue accumulation. These morphological alterations are associated to defects in the IGF1/Akt/mTOR pathway. Indeed, *Mecp2*-null muscles show downregulated levels of IGF1 and reduced phosphorylation of the ribosomal protein S6, suggesting that the hypotrophic phenotype is – at least in part – due to imbalance between protein synthesis and degradation. Since the conditional deletion of *Mecp2* from mouse skeletal muscle does not cause morphological or molecular defect in this tissue, we concluded that MeCP2 is not directly involved in the development and growth of skeletal muscle and that the observed muscular phenotypes displayed by *Mecp2*-null animals are mediated by non-cell autonomous mechanisms, probably through the paracrine/endocrine signalling of IGF1. Interestingly and in accordance with what reported by Cronk and colleagues, we also noticed an altered kinetics of expression of cytokines and macrophage markers in response to acute injury, which possibly contributes to disturb the skeletal muscle homeostasis in RTT.

### *1.2.3. Post-translational modifications dynamically regulate MeCP2 functional properties*

Beside the interactions of MeCP2 with functionally different partners deriving from its peculiar intrinsically disorganized structure, a complementary and fundamental level of regulation of MeCP2 multiple activities appears to be represented by post-translational modifications (PTM).

The first clues of MeCP2 PTM came from the observation that neuronal membrane depolarization leads to the production of an additional MeCP2 species that, on polyacrylamide gel, migrates slowly compared to the one classically found under basal

conditions (Chen et al., 2003). Sensory experience-dependent neuronal activation is essential for the refining of synapses and circuits during the postnatal brain development, when MeCP2 seems to be required and when RTT symptoms begin to manifest. This observation led to hypothesize that MeCP2 might sense neuronal activity therefore affecting circuits and synapses maturation (Cohen et al., 2011). This prompted the scientists to search for a possible dynamic regulation of the methyl-binding protein mediated by cellular stimulation.

Firstly, the mentioned slow-migrating form of MeCP2 was recognized as a result of phosphorylation (Chen et al., 2003); indeed, Serine-421 (S421; numeration refers to mouse Mecp2 isoform 2) was identified as phosphorylated upon neuronal stimulation and calcium influx (Zhou et al., 2006). Notably, despite the ubiquitous expression of MeCP2, S421 was found modified selectively in neural tissues, by a CamKII/CamKIV-mediated mechanism. In cultured neurons, phosphorylated S421 appeared to be selectively released from the *Bdnf* promoter, facilitating its activity-dependent transcription. Complementary, mutation of S421 to the non-phosphorylatable alanine significantly reduces the induction of *Bdnf* transcription upon membrane depolarization. Subsequently, it has been suggested that S421 phosphorylation affects dendrites and spine morphogenesis. Indeed, while the overexpression of wild-type *Mecp2* in cultured neurons leads to decreased dendritic branching, overexpression of S421A does not affect the dendrite complexity, therefore reinforcing the hypothesis that activity-dependent regulation of MeCP2 is critical for proper nervous system functions and highlighting a biological process with a high relevance for RTT pathogenesis (Chen et al., 2003; Zhou et al., 2006).

As logic consequence, a phospho-defective S421A knock-in (KI) mouse model has been generated (Cohen et al., 2011). Importantly, this mutation does neither alter the level of protein synthesis in the brain nor its nuclear localization, suggesting that S421 modification is not critical for directing the protein to chromatin. Cultured S421A cortical neurons show a significant increase in dendritic complexity and *in vivo* mutated pyramidal neurons are characterized by augmented branching of the distal apical dendrites, again suggesting the relevance of MeCP2 phosphorylation in neuronal architecture. Furthermore, scientists observed that in S421A cortical slices the balance between neural excitation and inhibition is shifted towards inhibition, resembling a phenotype also described in *Mecp2*-null mice. S421A animals do not manifest anomalies in their appearance, neither alterations in learning and memory tests nor major locomotor deficits; however, they show slightly impaired behavioural responses to novel experience that, in *MECP2* mutated patients, might contribute to the observed cognitive alterations. Finally, a global analysis of gene expression did not highlight

significant changes in S421A brain transcription. The overall mild phenotype of this KI mouse model might reflect the current absence of pathogenic mutations associated with this amino acid residue, suggesting that S421 phosphorylation controls only some aspects of circuit maturation (Bellini et al., 2014; Cohen et al., 2011). From a molecular point of view, the effects of activity-dependent S421 modification on the functions of MeCP2 are still debated. Indeed, while the first data indicated that phosphorylation of S421 precedes the detachment of MeCP2 from specific genes (such as *Bdnf*) and subsequent transcriptional activation, the ChIP-Seq analysis carried on by Cohen and colleagues revealed a genome-wide distribution of the phospho-S421 isoform of MeCP2. This approach showed that the profile of the protein binding to chromatin does not differ between resting and activated neurons, suggesting that phosphorylation at S421 doesn't induce the release of MeCP2 from DNA. It is possible that this modification induces chromatin remodeling and experience-dependent transcription by altering the interaction of the methyl-binding protein with its partners (Bellini et al., 2014; Cohen et al., 2011; Damen and Heumann, 2013).

Since mass spectrometry revealed that neuronal stimulation induces Mecp2 phosphorylation also at S424 in mouse brain (but not in rats), a double knock-in line carrying phospho-defective mutations at S421 and S424 has been generated (Li et al., 2011; Tao et al., 2009). In these mice, the mutant protein expression levels and intracellular localization are indistinguishable from the wild-type ones. *Mecp2*$^{S421A/S424A}$ animals have normal body weight, normal lifespan and do not show overt anomalies. Compared to wild-type littermates, they show increased locomotor activity. Moreover, they have better performance in behavioural tests that investigate hippocampus-dependent learning and memory capacities. Accordingly, long-term potentiation (LTP) is increased in hippocampal synapses of the mutated animals, together with excitatory synaptogenesis in both cortical and hippocampal primary neurons. At the molecular levels, *Mecp2*$^{S421A/S424A}$ brains show changes in transcription of genes (for example, the glutamate receptor 1 *Grm1*) important for the CNS functioning and also enhanced association to their promoters (Bellini et al., 2014; Li et al., 2011; Tao et al., 2009). These findings and the differences between the phenotypes of the double knock-in mouse and those of the S421A mutant highlight that the activities of MeCP2 could be regulated by the combination of several post-translational modifications.

To reinforce the idea that MeCP2 acts both as a sensor and an executor of different cellular stimuli, other PTMs have been described. In particular, the phosphorylation of S80 is highly conserved between humans, mice and rats. This modification is a vastly abundant event ubiquitously distributed throughout the brain. Contrary to S421 PTM, it occurs under resting

conditions, whereas neuronal stimulation decreases its levels. S80A knock-in mice have normal protein levels, normal lifespan and show slightly augmented body weight (Tao et al., 2009). Differently from what has been seen in *Mecp2*$^{S421A/S424A}$ animals, *Mecp2*$^{S80A}$ mice are characterized by decreased locomotor activity. No cross talk between S421 and S80 modifications has been detected, even if calcium influx is the trigger for both S421 phosphorylation and S80 dephosphorylation. S80 PTM does not affect the intracellular localization of Mecp2 and, *in vitro*, it increases the exogenous protein affinity for chromatin, with S80A mutation causing some gene transcription alterations in resting cells. Finally, the modification at this site seems to enhance the interaction between MeCP2 and the RNA-binding protein YB1. To conclude, it is conceivable that phosphorylation at S80 is important for MeCP2 regulation when neurons enter the resting state, possibly fine-tuning the protein-chromatin association and/or influencing the interaction between MeCP2 and its cofactors (Bellini et al., 2014; Gonzales et al., 2012; Tao et al., 2009).

Many other phosphorylation sites of MeCP2, such as S86, S149, S164, S229, S274, T308, S399 have been identified in mass spectrometry analyses, and many more can be predicted using computational tools (Figure 5A) (Bellini et al., 2014; Ebert et al., 2013; Gonzales et al., 2012; Tao et al., 2009). Among the ones experimentally identified, particularly interesting is the activity-induced T308 phosphorylation. Indeed, it occurs nearby R306, one of the most commonly mutated sites in Rett syndrome; it has recently been demonstrated that the R306C pathogenic alteration abolishes the interaction between Mecp2 and the N-CoR/SMRT corepressor complex in mice, causing severe RTT-like phenotypes (Lyst et al., 2013). Importantly, Ebert and colleagues demonstrated that the induction of T308 phosphorylation abrogates the interaction between MeCP2 and the N-CoR complex, reducing the repressive function of the protein TRD upon activity-induced target genes. On the contrary, the MeCP2 derivative in which this site has been mutated to the non-phosphorylatable alanine maintains the ability to interact with the N-CoR components. To investigate whether the loss of neuronal stimulation-dependent T308 PTM might be involved in RTT pathogenesis, a transgenic *Mecp2*$^{T308A}$ mouse line has been generated. This mutation does not alter the expression levels of Mecp2 and its binding to chromatin. Knock-in mice are characterized by reduced brain weight, hind limb clasping, motor deficits and an increased number of seizures compared to wild-type littermates. Moreover, they show alterations in the transcription of activity-induced genes. Altogether, these results underlie the relevance of the proper interaction between MeCP2 and N-CoR for the central nervous system functioning (Ebert et al., 2013).

From all these studies, it is possible to conclude that MeCP2 might dynamically perform different and sometimes opposite functions through the fine regulation obtained from different phosphorylation events (Figure 5A). However, we still lack information about how these modifications change during embryogenesis and throughout life. Moreover, we still don't know the majority of kinases and phosphatases involved in their dynamics and whether these PTMs occur in other cellular types beside neurons. Thus, a deeper characterization of MeCP2 phosphorylation is required to answer these questions and to reveal the mechanisms by which it regulates the methyl-binding protein biological activities.

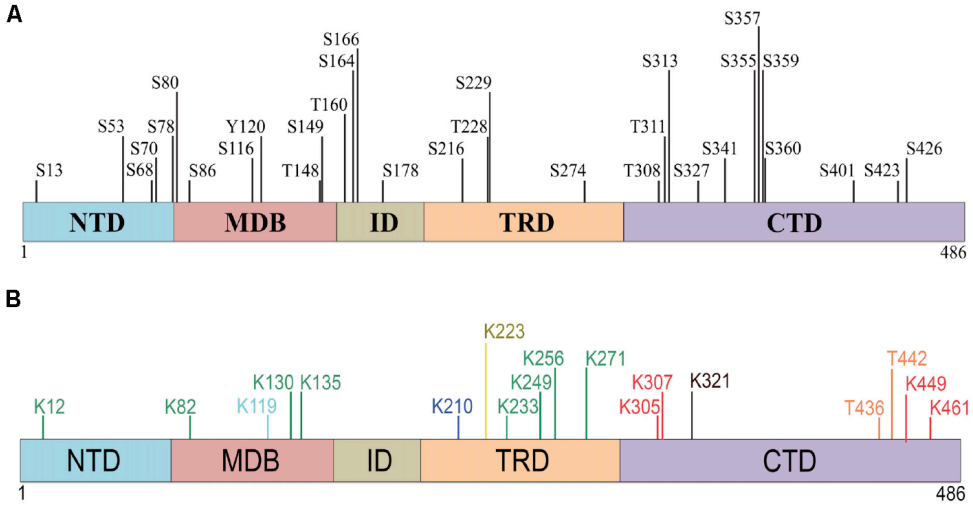


**Figure 5. MeCP2e2 post-translational modifications.** A) Phosphorylation sites on Mecp2; B) PTMs other than phosphorylation on the Mecp2 sequence. Green: ubiquitination; blue: methylation; red: acetylation; yellow: SUMOylation; orange: O-glycosilation; black: ubiquitination and acetylation; cyan: ubiquitination and methylation. Adapted from (Bellini et al., 2014).

Finally, even if data are still incomplete and no mouse models have been generated so far, others post-translational modifications different from phosphorylations have been demonstrated to contribute to the described MeCP2 "regulatory code" (Figure 5B). In particular, *in vitro* exogenously expressed MeCP2 presents ten ubiquitination sites, mainly localized in the MBD and TRD, which may be involved in the control of both rapid protein degradation and trafficking. Notably, three of these sites are affected by RTT pathogenic missense mutations. Interestingly, MeCP2 also contains two highly conserved PEST motives (enriched in proline, glutamate, serine and threonine). These sequences are usually destabilized by protein modifications leading to proteolytic degradation by the ubiquitin-proteasome system. Therefore, it is possible that the PEST domains and their PTMs could be relevant for maintaining the correct levels of MeCP2. Moreover, several residues have been reported as modified by the small ubiquitin-like modifier (SUMO), as

acetylated, methylated or O-glycosilated (Bellini et al., 2014; Gonzales et al., 2012). Future studies are required to better characterize the full spectrum of MeCP2 post-translational modifications and their possible involvement in the pathogenesis of *MECP2*-related disorders.

### *1.2.4. Tyrosine-120 phosphorylation: the rationale of our project*

Given the probable relevance of PTMs for MeCP2 activities throughout life, we reasoned that studies aiming at investigating novel protein modifications should focus on sites conserved by evolution and/or found mutated in RTT patients. This approach would possibly provide important information about the physiological and pathological mechanisms regarding the methyl-binding protein.

Going through the literature, we noticed that in 2008 MeCP2 Tyrosine-120 (Tyr-120) was for the first time identified as phosphorylated in HeLa cells during mitosis (Dephoure et al., 2008). Importantly, the highly conserved Tyr-120 amino acid was previously associated with Rett syndrome. Indeed, in 2001 it was found mutated in a Japanese three-years old girl, who was affected by several symptoms such as deceleration of head growth, loss of acquired skills, social withdrawal and stereotypic hand movements. This patient was carrying a Y120D tyrosine to aspartic acid substitution, a kind of modification that is often regarded as mimicking a constitutive phosphorylation state (Inui et al., 2001).

These data have prompted our laboratory to investigate this novel event of phosphorylation *in vitro* and *in vivo* in order to understand its biological relevance and the pathogenic consequences of the alteration of the Tyr-120 site.

Regarding the *in vitro* characterization, in a recently published work from our lab (Bergo et al., 2015), MeCP2 Y120 phosphorylation was reported in different cell types. It was as well confirmed that Tyr-120 PTM is enriched during mitosis. Importantly, immunofluorescence analyses performed on HeLa cells showed that this phospho-isoform localizes at the centrosome with a cell cycle-regulated pattern. Indeed, during interphase, even if the Y120(P) signal prevalently recognizes nuclear puncta, an initial colocalization between this isoform and the centrosomal-marker γ-tubulin is already detectable. During mitosis, the centrosomal Y120(P) signal increases up to metaphase. During anaphase it strongly decreases and becomes undetectable in telophase. Notably, as for the total MeCP2 protein, the colocalization between the phospho-isoform and centrosomal markers was identified also in glial cells and in post-mitotic cultured neurons. Biochemical approaches suggested that the

pathogenic Y120D mutant has a stronger affinity for the centrosome and/or a longer localization at this organelle. Moreover, while re-expression of the wild-type protein ameliorates the already mentioned proliferation defect seen in MeCP2-depleted cells, expression of the Y120D construct does not rescue this phenotype, underling the necessity of a normal Tyr-120 residue for the newly described proliferative function of MeCP2 (Bergo et al., 2015).

Concomitantly, the *in vivo* analysis has led to the generation of a novel knock-in mouse model bearing the Y120D mutation, that represents the focus of the studies herein presented. To the best of our knowledge, this is the first time in which an amino acid residue that is both found altered in RTT cases and post-translationally modified is modelled *in vivo*.

# 2. Materials and Methods

## 2.1. Animal husbandry

The knock-in Y120D mouse line was obtained as described in the 2.1 section "*Generation of the Y120D mouse line*". Animals were housed in the animal facility of the San Raffaele Scientific Institute of Milan. KI males, heterozygous females and WT controls (of both the C57BL6J and CD1 background) were obtained by crossing heterozygous females with WT males.

The DNA of the first KI mice generated was sequenced, to confirm the presence of the single point mutation. A fragment of the modified *Mecp2* region was amplified from genomic DNA using the two specific primers:

- Primer COM: 5' – CAG GGC CTC AGA GAC AAG C – 3'
- Primer KI REV: 5' – GGG TTA ATT GAT ATC CAA TTG GGA TCC – 3'

The following PCR protocol was used:

- Mix
  - *Pfu* Buffer (Promega): 1X
  - PCR Nucleotide Mix (Promega): 200 µM
  - Primer COM: 1 µM
  - Primer KI REV: 1 µM
  - *Pfu* DNA Polymerase (Promega): 1.25 Units
  - Genomic DNA: 1 µl
  - $H_2O$ to a final volume of 50 µl
- Program
  - Heat Lid 110°C
  - 95°C 2min
  - Start Loop: 35 cycles
    - 95°C 30 sec
    - 60°C 30 sec
    - 72°C 1 min
  - Close Loop
  - 72°C 5 min

Subsequently, 1 µl (5 U) of XtraTaq (Genespin) was added to the mix, then incubated at 72°C for 30 min to obtain DNA fragments with 3'-overhanging A nucleotides. Thus, DNA was TA cloned into the pGEM-T Easy vector (Promega) using the following ligation protocol:

- Mix
    - Rapid Ligation Buffer (Promega): 1X
    - pGEM vector (Promega): 50 ng
    - Insert: 30 ng (1:3 vector:insert ratio)
    - T4 DNA ligase (Promega): 1 µl (3 U)
    - $H_2O$ to a final volume of 10 µl

    1 h at 37°C

The obtained clones were sequenced by Eurofins Genomics Srl, using universal SP6 and T7 primers.

Genotyping was performed with the already mentioned Primer COM and KI REV *plus* the Primer WT REV (5' – GCA GAT CGG CCA GAC TTC C – 3') and the following PCR protocol:

- Mix
    - Buffer with $MgCl_2$ (Genespin): 1X
    - PCR Nucleotide Mix (Promega): 200 µM
    - Primer COM: 1 µM
    - Primer KI REV: 1 µM
    - Primer WT REV: 1 µM
    - XtraTaq Polymerase (Genespin): 5 U
    - Genomic DNA: 2 µl
    - $H_2O$ to a final volume of 20 µl
- Program
    - Heat Lid 110°C
    - 95°C 2min
    - Start Loop: 35 cycles
        - 95°C 30 sec
        - 60°C 30 sec
        - 72°C 1 min
    - Close Loop
    - 72°C 5 min

Fragments were separated on 2% agarose gel, stained with SYBR-Safe and visualized under

UV light. The PCR gave rise to a 550 bp product specific for the KI allele and to a 300 bp product for both the WT and KI ones.

Animals were sacrificed – at the different ages indicated along the *Results* and *Figure Legends* sections – by cervical dislocation and then organs were harvested and immediately weighted.

## 2.2. Phenotypic characterization of the mouse model

KI mice and WT littermates were evaluated following the scoring system described by Guy and colleagues (Guy et al., 2007), with some variations. Indeed, to better represent the phenotypical variability of the animals, we introduced – in addition to the 0, 1 and 2 scores given by Guy – the intermediate 0.5 and 1.5 scores. At each scoring session mice were weighed and scores were given as follows:

- General condition: coat condition, eyes tidiness and presence of wounds were evaluated. 0: no differences between WT and KI, coat is bright and groomed, eyes are clean, no wounds are present. 0.5: with respect to the WT control coat is less shiny or tidy OR eyes are less clean OR small wounds on the mouse body or tail are present. 1: coat is ungroomed or dull or dirty OR eyes are dull OR wounds are evident OR two of the 0.5-scored phenotypes are present together. 1.5: spot without fur evident and coat ungroomed/dull OR two of the 1-scored phenotypes present together. 2: piloerection together with large alopecia OR eyes crusted OR extended and serious wounds.
- Mobility: the mouse is placed on the bench and let free to move, the spontaneity of the movements and the time spent not moving are evaluated. 0: as WT. 0.5: the mouse does not move immediately when let free, but evidently requires more time than the control to start its movements OR movements are less quick. 1: mouse movements are slow and/or interrupted by freezing periods. 1.5: mouse starts to move only in response to a prod or when encouraged with a food pellet placed nearby and spends long periods immobile. 2: no movements when placed on the bench (anyway mice may become active when in their cage).
- Hind limb clasping: the mouse is held for the tail and maintained suspended for 30 seconds. 0: legs are large and splayed outwards. 0.5: one leg is drawn to the body in a discontinuous manner. 1: one leg is firmly drawn in to the body OR both legs are drawn to the body towards each other, but discontinuously. 1.5: both legs are firmly drawn to the body, without touching each other. 2: both legs are tightly drawn to the

body, touching each other.

- Tremor: mouse is placed on the palm of the hand. 0: no tremor. 0.5: slight basal tremor OR long periods without tremor interspersed with sporadic events of mild tremor. 1: basal tremor OR intermittent events of mild tremor. 1.5: prolonged events of tremor interspersed with moment in which a basal tremor is present. 2: continuous tremor OR almost continuous violent tremor.

Importantly, animals scoring 2 for the general condition or tremor category were euthanized for ethical reasons. Day of euthanasia was considered the day of death, without distinguishing it from natural death.

Graphically, for each parameter the evolution of symptomatology was represented through a cumulative plot, obtained by plotting for each day of evaluation the animal score for that day summed to all the preceding scores (in Figure 7D, 8C and 9 these data are represented as the mean of WT and KI values). For statistical analyses, the Student's *t* test was applied to the pure/not cumulated scores recorded at each time point.

## 2.3. Histology

Animals were deeply anesthetized with Avertin (Sigma-Aldrich) and transcardially perfused with 4% paraformaldehyde (PFA). Brains were post-fixed in PFA 4% for additional 3 hours, cryoprotected overnight in 30% sucrose in PBS, embedded in O.C.T. Compound (Tissue-Tek) using cooled isopentane and then stored at -80°C. Tissues were sagittaly sectioned with a cryostat (Leica) to obtain 40 µm free-floating sections, which were conserved in a cryoprotectant solution (300 ml Ethylene glycol, 300 ml Glycerol, 1.57 gr monobasic sodium phosphate, 5.45 gr dibasic sodium phosphate, $H_2O$ to a final volume of 1 litre) at -20°C. To perform Nissl staining sections were mounted on microscope slides and hydrated by rapidly passing through a series of ethanol solutions (100%>95%>75%>50%). After washing 2x1 min with $H_2O$, sections were incubated with the Cresyl Violet solution (1.25 gr Cresyl Violet [Sigma-Aldrich], 0.75 ml glacial acetic acid, $H_2O$ to a final volume of 250 ml) for 7 min and washed 1 min with $H_2O$. Then, excess of staining solution was removed and sections were dehydrated by rapidly passing through a series of ethanol solutions (50%>75%>95%>100%) and, finally, into 100% Xylene. Eventually, slices were mounted with DPX. Images were taken with a Leica DM IRB microscope, coupled to a Zeiss Camera, at 5X magnification. To evaluate thickness of the frontal cortex, we used brain medial sections recognizable by the hippocampal formation. To measure roughly the same cortical areas, we placed over the

images a grid so that its initial vertical line was tangential to the most rostral part of the corpus callosum. The grid was made of 8 column/"position", each 250 μm wide. We measured cortical thickness (from layer II to layer VI) in the middle of each of these columns, using the analyser software ImageJ. To minimize the experimental variability measurements of the 8 positions were mediated in 3 groups (1-3, 4-6, 7-8).

## 2.4. Neuronal cell culture

Primary cultures of cortical neurons were prepared from E17 mouse embryos. Cortices were isolated under a dissection microscope, washed three times in HBSS (Gibco-Life Technologies), digested with Trypsin 0.25% (Gibco-Life Technologies) at 37°C for 7 min, washed three times in HBSS and, then, mechanically dissociated in dissecting medium (DMEM [Sigma-Aldrich], 10% Horse Serum, Glutamine 1% [Sigma-Aldrich]). Cells were diluted in the neuronal culture medium (containing Neurobasal [Gibco-Life Technologies], 2% B-27 [Gibco-Life Technologies], Glutamine 1% [Sigma-Aldrich]) and plated in 12-multiwell plates on glass coverslips precoated with 0.1 mg/ml poly-L-lysine (Sigma-Aldrich) at a density of 30000 cells/well. Neurons were grown in the neuronal culture medium that was never changed.

## 2.5. Immunofluorescence

Neurons cultured on coverslips – at the DIV indicated along the *Results* and *Figure Legends* sections – were washed with PBS and fixed in 4% PFA for 20 min a room temperature (RT). After washing 4x5min with PBS, cells were permeabilized for 10 min with 0.1% Triton X-100 in PBS, washed 2x5min with PBS and incubated for 1 hour at RT in blocking solution (10% horse serum [Euroclone], 0.1% Triton X-100 [Sigma-Aldrich] and PBS). Cells were then incubated with the primary antibody diluted in blocking solution overnight at 4°C. Primary antibodies used were: rabbit anti-Mecp2 (1:100, Cell Signaling, D4F3) and mouse anti-TuJ1 (1:2000, Sigma-Aldrich). Cells were then washed 8x10min with PBS and incubate with the appropriate fluorescent secondary antibody (AlexaFluor 488 anti-rabbit or anti-mouse, diluted 1:500 in blocking solution) for 1 hour at RT. After washing 2x5min with PBS, cells were counterstained with DAPI (Invitrogen) for 10 min at RT, washed 2x5min with PBS and mounted in Prolong Gold (Invitrogen). Images were taken at 40X and 100X

magnification using Zeiss microscopes. The size of neuronal nuclei was evaluated with ImageJ by measuring the DAPI-stained area of each nucleus.

## 2.6. qPCR

Total RNA was purified from mice cortices using the RNeasy Mini Kit (QIAGEN) as instructed by the manufacturer. Extracted RNA was quantified with NanoDrop and its quality was assessed through a denaturing 1% agarose gel with Ethidium Bromide. Complementary DNA (cDNA) was transcribed using the RT2 First Strand Kit (QIAGEN) according to the manufacturer's instructions. PCR reactions were run on a StepOnePlus Real-Time PCR System (Applied Biosystems), using SYBR Select Master Mix (Applied Biosystems) 1X and primers 0.4 μM. All samples were evaluated in triplicate. ΔCt were calculated using 18S as normalizer. Gene expression is represented as relative to the WT one.

- Primers:
  - *Mecp2*:
  - Fwd: 5' AAACCACCTAAGAAGCCCAAATC 3'
  - Rev: 5' TTGACAACAAGTTTCCCAGGG 3'
  - *Bdnf*:
  - Fwd: 5' AAGTCTGCATTACATTCCTCGA 3'
  - Rev: 5' TTATCAATTCACAATTAAAGCAGCAT 3'
  - *Hif1α*:
  - Fwd: 5' GCTGAAGACACAGAGGCAAA 3'
  - Rev: 5' TACTTGGAGGGCTTGGAGAA 3'
  - *18S*:
  - Fwd: 5' GTAACCCGTTGAACCCCATT 3'
  - Rev: 5' CCATCCAATCGGTAGTAGCG 3'

## 2.7. Western Blot

Whole brains and brain areas harvested from WT and KI mice were mechanically homogenized in lysis buffer (50mM Tris-HCl pH 7.4, 500 mM NaCl, 1% Triton X-100, 2 mM EDTA, 1 mM DTT, 1X PhosSTOP [Roche], 1X cOmplete EDTA-free protease inhibitor cocktail [Roche], $H_2O$) using a Potter homogenizer. Lysates were incubated 30 min on ice and

sonicated (for 5 min + 5 min + 3 min, amplitude 100%). After a 15 min centrifugation at 13000 rpm at 4°C supernatants were collected and proteins were quantified with Pierce BCA Protein Assay Kit (Thermo Scientific).

Protein were electrophoresed on 10% SDS-polyacrylamide gel, blotted onto nitrocellulose using the Trans-Blot Turbo Transfer System from Bio-Rad (11 min, 2.5 A, 25 V), blocked for 30 min with 5% milk in TBST1X and probed overnight at 4°C with the following primary antibodies: rabbit anti-Mecp2 (1:1000, Sigma-Aldrich); mouse anti-Tuj1 (1:10000, Sigma-Aldrich); rabbit anti-P-Ser164 (1:1000, Covance); rabbit anti-phospho S6 ribosomal protein (1:1000, Cell Signaling, Ser240/244); rabbit anti-S6 ribosomal protein (1:1000, Cell Signaling, 5G10); rabbit anti-H1 (1:1000, GeneTex). Membranes were then incubated with the appropriate fluorescent secondary antibodies AlexaFluor 488 (1:2000) or with the HRP-conjugated ones (1:10000, Cell Signaling). Bands were either detected and visualized using the fluorescence laser scanner Typhoon FLA 9000 (GE Healthcare) or using a chemiluminescence-based detection system (SuperSignal West Pico Chemiluminescent Substrate, Thermo Scientific). When both rpS6 and P-rpS6 expression had to be evaluated, we firstly used the antibody directed against the phospho-isoform: after having detected its signal, we stripped it (stripping solution: 60 mM Tris-HCl pH 8.6, SDS 1%, β-mercaptoethanol 7µl/ml) and the membrane was probed with the anti-S6 ribosomal protein antibody. For quantitative measurement, blots were analyzed with ImageJ, normalizing band intensities to TuJ1 or rpS6 levels. To evaluate Ser164 phosphorylation we made a ratio between the normalized phospho-protein and the normalized total isoforms of Mecp2. Protein levels are represented as relative to the WT ones.

## 2.8. Mecp2 salt extraction assay

Brains were mechanically lysed in the cytosol lysis buffer (10 mM Hepes pH 7.5, 1.5 mM $MgCl_2$, 10 mM KCl, 0.2% NP40, 0.1 mM EDTA, 10% Glycerol, 1X PhosSTOP [Roche], 1X cOmplete EDTA-free protease inhibitor cocktail [Roche], $H_2O$), on ice, using a Potter homogenizer. Samples were incubated 30 min on ice and centrifuged at 2000g for 5 min at 4°C. Supernatants were collected and kept as the cytosolic fraction. The nuclear pellets were resuspended in a buffer containing 10 mM Tris-HCl pH 7.4, 1X PhosSTOP, 1X cOmplete EDTA-free protease inhibitor cocktail and $H_2O$, supplemented with 200 mM NaCl. These samples were vigorously vortexed and incubate on ice for 20 min, then they were centrifuged at 2000g for 5 min at 4°C. Supernatants were collected and conserved. This procedure was

repeated for other 5 times, supplementing the buffer with increasing concentrations of NaCl (300 mM – 400 mM – 500 mM – 600 mM – 700 mM). Finally, equal volumes of each fraction were loaded on 10% SDS-polyacrylamide gel to assess by WB the extraction of the protein of interest. The pattern of H1 extraction was evaluated as control of the experimental procedure.

## 2.9. Chromatin accessibility to MNase

Brains were mechanically lysed using a Potter homogenizer on ice, in buffer A (0.25 M sucrose, 60 mM KCl, 15 mM NaCl, 10 mM MES pH 6.5, 5 mM $MgCl_2$, 1 mM $CaCl_2$, 0.5% Triton X-100, 1X PhosSTOP [Roche], 1X cOmplete EDTA-free protease inhibitor cocktail [Roche], $H_2O$), which allows the maintenance of intact nuclei. Samples were incubated on ice for 10 min and then centrifuged at 7000 rpm for 10 min at 4°C. Supernatants were discarded and pellets were washed with buffer A. After a 5 min centrifugation at 7000 rpm at 4°C, supernatants were again discarded. Nuclear pellets were resuspended in the digestion buffer B (50 mM NaCl, 10 mM Pipes pH 6.8, 5 mM $MgCl_2$, 1 mM $CaCl_2$, 1X PhosSTOP, 1X cOmplete EDTA-free protease inhibitor cocktail, $H_2O$). The number of nuclei was counted with the Burker chamber and samples were diluted in buffer B in order to have a final concentration of 200000 nuclei/µl. 50 µl of samples were taken, supplemented with 3 µl of 0.5 M EDTA and conserved as the undigested fractions. The remaining samples were pre warmed at 37°C and then 10 Units of MNase (Worthington) every $40x10^6$ nuclei were added. Samples were digested for 20 minutes. Intermediate fractions were collected at 2.5 min, 5 min, 7.5 min, 10 min and 20 min. MNase digestion was stopped by adding 3 µl of 0.5 M EDTA to each fraction. DNA was extracted from the different fractions (using Phenol/Chloroform) and quantified with NanoDrop. For every fraction 10 µg of DNA were loaded on a 2% EtBr agarose gel, which was run for approximately 5 hours, in order to visualize the digested DNA bands. For each gel lane a densitometry plot was obtained using the ImageJ software. Then, plots of WT and KI samples at the same time point were superimposed to better identify possible differences in their digestion.

# 3. Results

## 3.1. Generation of the Y120D mouse line

The KI targeting construct, bearing the DNA point mutation (T>G) that leads to the tyrosine to aspartic acid substitution, was produced by the Gene Bridges Company. Briefly, the modification of the *Mecp2* genomic locus was obtained by multi-site Red/ET recombination as follows (Figure 6A). Two overlapping DNA fragments harbouring i) a portion of the exon 3 of *Mecp2* containing the point mutation of interest and a portion of the Neomycin resistance cassette and ii) the entire Neomycin cassette (that is two FRT site flanking the PGK/gb2 promoter and the Kanamycin and Neomycin resistance genes) were amplified through PCR from a synthetic DNA fragment and a Gene Bridges plasmid, respectively. Then, these DNA portions were co-electroporated into the *E. Coli* strain HS996, which contains the pRed/ET expressing plasmid and a BAC harbouring a part of the *Mecp2* genomic locus. Addition of L-arabinose to the culture at a temperature of 37°C induced Red/ET recombination, allowing the insertion in the BAC of the mutated exon and of the Neomycin cassette between two flanking *Mecp2* homology arms of 6 kilobases (kb) each. Culture was then plated on Kanamycin-containing LB agar and sequencing of the resistant clones confirmed the precise basepair mutation and the integrity of all the functional elements. Finally, the modified *Mecp2* genomic locus was subcloned into a high-copy plasmid backbone (Figure 6B). The obtained plasmid DNA was again subjected to sequencing to confirm the integrity of the different elements and junctions and the correct modification of the *Mecp2* exon 3.

Subsequently, at the Institute of Molecular Oncology (IFOM) in Milan, the linearized construct was transfected into embryonic stem cells (ESC) of the 129 mouse strain. The ESCs that had incorporated the mutant DNA were positively selected exploiting the presence on the KI construct of the Neomycin resistance cassette. Cells in which homologous recombination had taken place, leading to the substitution of the wild-type genomic locus with the targeted one, were screened through Southern Blot (*data not shown*). The selected genetically modified embryonic stem cells were then microinjected into the blastocysts retrieved from a C57BL6J female. Subsequently, the blastocysts were implanted in the uterus of a foster C57BL6J pseudo-pregnant mother. The chimerism of the born mice was recognized by the colour of their fur: chimeric males were mated with C57BL6J wild-type females, giving rise to the first generation (N1) of female mice heterozygous for the modified allele. The effective presence of the point mutation in these animals was confirmed by DNA sequencing (Figure

6C). The subsequent generations were obtained by mating heterozygous KI females with wild-type C57BL6J males and the presence of the construct bearing the Y120D missense mutation was verified by PCR genotyping (*see the Materials and Methods section*).

To firstly investigate whether the targeting of the *Mecp2* genomic locus affected or not the gene transcription, we analysed *Mecp2* mRNA expression in the cortex of third-generation KI males at P30 and we didn't observe any significant difference with respect to the control wild-type (WT) littermates (Figure 6D), thus confirming that gene functional elements are intact.

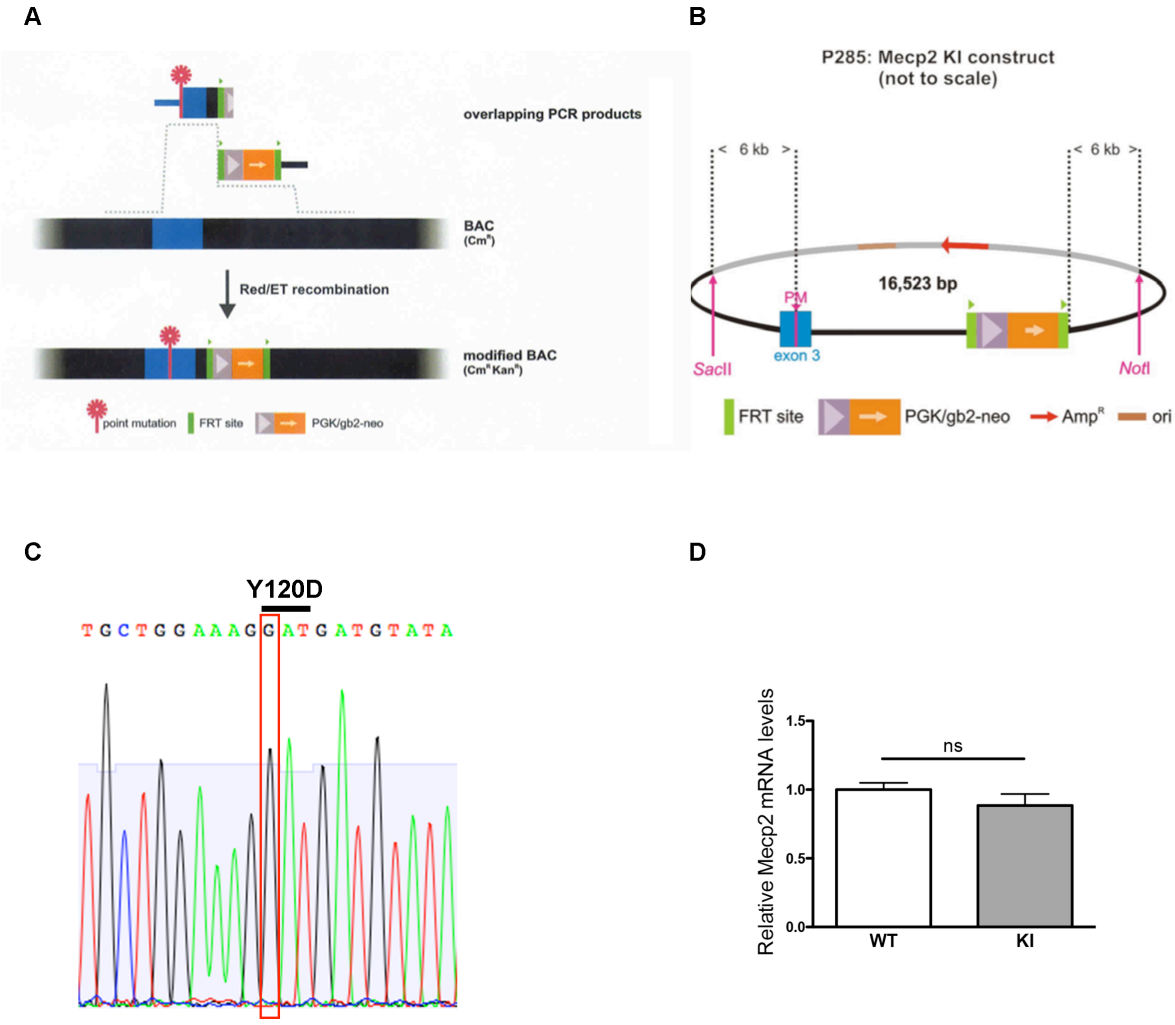


**Figure 6. Generation of the Y120D mouse line.** A) Modification of the *Mecp2* genomic locus by Red/ET recombination between two DNA fragments bearing the mutated exon 3 and the Neomycin resistance cassette and the BAC containing a part of the *Mecp2* gene. Blue: exon 3; black: *Mecp2* genomic locus. B) Final *Mecp2* construct harbouring the desired point mutation. Grey: high-copy plasmid backbone; black: *Mecp2* genomic sequence; pink: unique restriction sites used for the construct linearization; dashed lines underlie the 6 kb *Mecp2* homology arms flanking exon 3 and the Neomycin resistance cassette. C) DNA sequencing results showing the presence in the generated animals of the single point mutation T>G – highlighted in red – that leads to the Tyr-120 mutation into aspartic acid. D) *Mecp2* mRNA expression in the cortex of WT and KI male mice at P30 (n=3). Data are represented as mean±s.e.m. Significance is calculated with Student's *t* test (ns = not significant).

## 3.2. Phenotypic characterization of the Y120D mouse model

### *3.2.1. The C57BL6J KI colony*

We transferred the generated mice to the San Raffaele animal house and we started to evaluate the features of the colony.

We firstly noticed that the presence of the mutated allele does not cause embryonic death, since the percentage of WT and KI animals born is not statistically different (54,63% WT *versus* 45,37% KI; *p*-value = 0,336; Chi square = 0,926; degree of freedom [d.f.] = 1).

Y120D male mice have a reduced, even variable, lifespan; indeed, they die (or they are euthanized for ethical reason) between 2 and 5 months of age, with the average time of death being P103. On the contrary, the heterozygous mutant females live longer than males, reaching more than 10 months of ages.

Macroscopically, KI males always appear smaller compared to the WT littermates, whereas mutated females tend to become obese. Therefore, we decided to assess the whole body and organs weights of fully adult mice at their death. The total weight of KI males (Figure 7A) resulted significantly diminished compared to the WT controls (sacrificed at the same age), with a 34,60% reduction. A similar reduction (35,74%) is also observed for the Y120D muscles, which therefore possibly represent the major contributors to the overall body weight decrease. Heart and kidney tend to have a diminished weight compared to the controls, but this difference is not significant. Finally, brains harvested from the KI males statistically weigh less (15,70%) than the WT ones. It remains to be clarified whether the reduction in brain size is a consequence of the overall decrease in body weight or whether it is directly caused by the presence of the Y120D protein in the central nervous system. Interestingly, the reduction values here reported for brain, gastrocnemius and total weight are similar to the ones we reported for the *Mecp2*-null mice in (Conti et al., 2015). Differently from what seen in males, heterozygous adult (more than six months of age) females weigh largely more than the controls (Figure 7B,C), having a significant increase of 66,90% with respect to the WT mice. Since during the dissection procedures we noticed a great amount of subcutaneous adipose tissue in KI females, we hypothesize that this is the main cause of the total weight increase reported. Eventually, brains from Y120D females are slightly and not significantly reduced in size compared to the WT ones.

Subsequently, we evaluated whether the Y120D pathogenic mutation induces gross behavioural and phenotypical alterations in knock-in mice. For this purpose, we exploited the

already published scoring system used for the characterization of the first model of *Mecp2* postnatal re-activation (Guy et al., 2007) (*see the Materials and Methods section*). We firstly characterized the KI males, since – as already described – they don't show the confounding effects deriving from the X-chromosome inactivation phenomenon. Their evaluation started at P29 and was performed twice a week (Figure 7D).

A

| Males | total weight | brain | heart | kidney | gastrocnemius |
|---|---|---|---|---|---|
| WT (gr) | 26,663 ± 1,269 | 0,418 ± 0,011 | 0,135 ± 0,007 | 0,160 ± 0,004 | 0,153 ± 0,009 |
| KI (gr) | 17,423 ± 1,273 | 0,352 ± 0,004 | 0,110 ± 0,016 | 0,120 ± 0,013 | 0,098 ± 0,005 |
| Reduction vs WT (%) | 34,60 | 15,70 | 18,50 | 25,00 | 35,74 |
| Significance | *** | *** | ns | ns | ** |

B

| Females | total weight | brain |
|---|---|---|
| WT (gr) | 29,207 ± 1,155 | 0,410 ± 0,025 |
| KI (gr) | 48,770 ± 2,052 | 0,374 ± 0,005 |
| Increase vs WT (%) | 66,90 | -8,78 |
| Significance | *** | ns |

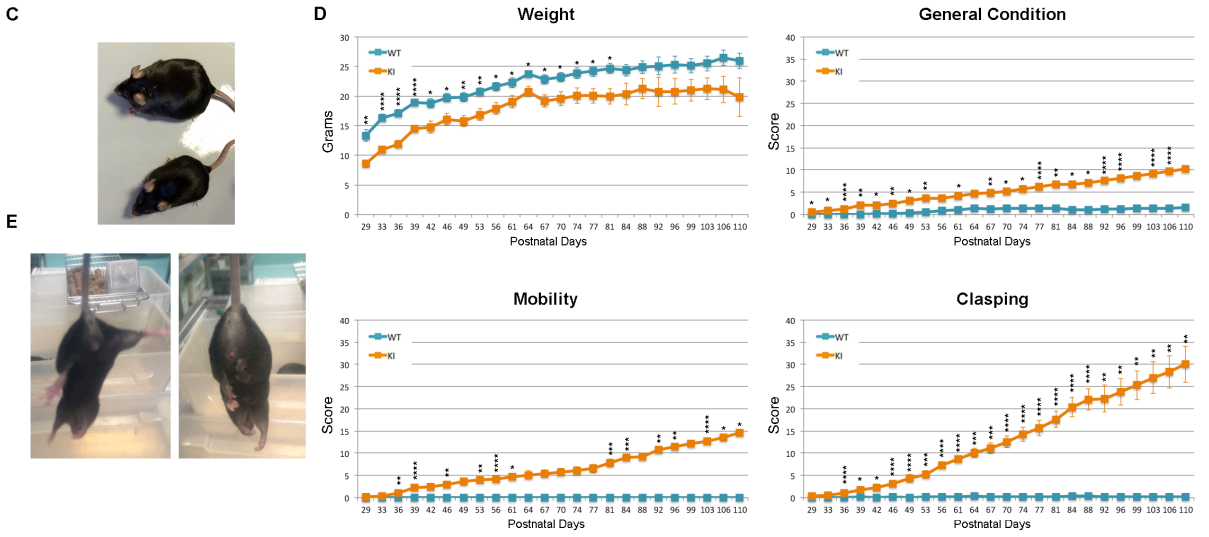


**Figure 7. Phenotypic characterization of the C57BL6J Y120D mouse model.** A and B) Measures of the total body and organs weight of WT and KI males (A) or WT and KI females (B) at their sacrifice (n=4 to 7 and 3 to 6, respectively). Data are represented as mean±s.e.m. Tables also report the percentage of weight reduction/increase calculated considering WT values as 100%. Significance is calculated with Student's *t* test (*p*-value: **<0.01; ***<0.001). C) Representative picture of an heterozygous KI female (*top*) and its WT control (*bottom*) at P250. D) Plot of total body weight and cumulative phenotypic score profiles of WT and KI male mice, showing the progression of RTT-like symptoms in the Y120D animals (n=7 WT and 6 KI at the beginning of the testing period). Data are represented as mean±s.e.m. Significance is calculated with Student's *t* test, which is performed on the pure (not cumulated) scores at each time point (*p*-value: *<0.05; **<0.01; ***<0.001; ****<0.0001). E) Representative picture of an adult KI male (*right*) doing hind limb clasping (on the *left* there is its WT control).

For what concerns the progression of the body weight, already at P29 the KI mice weighed approximately 4 grams less than control littermates and this discrepancy was maintained in a quite constant manner throughout all the testing period. From P84 onwards, the difference between WT and KI is no more significant probably because the number of animals tested is decreasing due to the KI deaths. Compared to WT littermates, the general conditions of KI

animals were slightly but significantly worse since the first evaluations. Their coat was dull and ungroomed, although eyes were clean. Sometimes they showed uneven wearing of the teeth or flattened posture. Spontaneous movements were slightly impaired since approximately 40 days of life; generally this phenotype became more prominent in the days before the mutant mice euthanasia, with the animals spending long periods freezed on the bench or not moving at all. The initial reduction in spontaneous movements coincided with the first manifestations of hind limb clasping from the Y120D mutants (Figure 7E). This represents the most evident and progressive symptom: the 100% of the KI males displayed it from around 7 weeks of age and it reached the highest values on the cumulative score scale compared to the other features tested.

Differently from what described in (Guy et al., 2007), we didn't manage to evaluate tremors in our set of animals, since the otherwise normal WT control constantly manifested perceivable tremors during the testing period.

Given these observations, we concluded that our new mouse model suffers from multiple symptoms related to the mutation of the Tyrosine-120 residue.

As for the *Mecp2*-null mouse model, Y120D males appear infertile. Testes of the KI mice are external and the causes of their infertility are still unclear. Thus, heterozygous females are necessary for the maintenance and expansion of the colony, which actually proceeds very slowly. For this reason, at the time being, we haven't characterized the phenotypic alterations of Y120D females yet. The difficulties in the maintenance of this mouse line are ascribable to four main factors already encountered with the handling of the *Mecp2*-null C57BL6J colony, that is: i) heterozygous females give rise to small litters, ii) sometimes they do not take care of their pups or iii) they cannibalize them, iv) the percentage of matings that results in pregnancy is low (roughly 30% for Y120D females). Importantly, all these drawbacks appear to worsen with the generation number, rendering quite difficult to continue the studies in this genetic background. On the other hand, in our laboratory it has recently been demonstrated that the CD1 background represents a valid alternative to the commonly used C57BL6J model for the *in vivo* study of *Mecp2* mechanisms (Cobolli Gigli et al., *paper under revision;* Bedogni et al., 2015). Indeed, compared to the C57BL6J ones, CD1 *Mecp2*$^{+/-}$ females usually generate larger litters and take better care of their progeny, without cannibalizing the pups. CD1 *Mecp2*-null males are characterized by prolonged lifespan and by a slightly delayed onset of RTT symptoms with respect to the C57 mice. Therefore, they appear more robust but, importantly, they recapitulate most of the behavioural, morphological and molecular phenotypes of the

C57 *Mecp2*-null animals. In conclusion, the maintenance of the *Mecp2*-null line on the CD1 background make the handling of the colony easier, without affecting the validity of the mouse model for the study of RTT pathogenic mechanisms (Cobolli Gigli et al., *paper under revision*). We speculated that this could be true also for our Y120D KI model and therefore we transferred the mutated allele into the CD1 background, by crossing heterozygous C57 females with wild-type CD1 males and backcrossing the progeny with the same strategy used for the C57 strain. Thus, we obtained mutated CD1 animals that we phenotypically characterized and that we employed in place of the C57 ones when the latters' number was too small.

### *3.2.2. The CD1 KI colony*

As for the C57 strain, we noticed that the mutated allele does not lead to embryonic death in the CD1 line. Indeed, WT and KI mice were equally represented in the progeny (50,29% WT *versus* 49,71% KI; *p*-value = 0,940; Chi-square = 0,006; d.f. = 1).

At P18 (Figure 8A) Y120D CD1 males are significantly underweight compared to control littermates (reduction of 30,03%). Moreover, they already show a 12,16% reduction in the weight of their brains. At P40 (Figure 8B) the difference in total body weight between the two genotypes is smaller than at P18 (13,12%), while, interestingly, the reduction in brain weight is maintained, with a value (15,02%) that resembles the one observed in the adult C57 males. KI muscles have a weight reduction (14,29%) that – even if not significant – is similar to the one of the total body. Finally, also heart and kidney are reduced in size at this time.

We followed the progression of the CD1 Y120D males' phenotypical alterations with the same approach we used for the C57 mutants. The evaluations started at around one month of age and were performed once every seven/ten days (Figure 8C). As expected, the total body weight was initially reduced in the KI animals. However, they soon reached the WT levels and overcame them between the second and third month of life, becoming overweight. This discrepancy between what observed in C57 and CD1 total body weight progression is in accordance with previous works reporting that this parameter is dependent on the genetic background (Cobolli Gigli et al., *paper under revision*; Ricceri et al., 2008). For what concerns their general conditions, Y120D CD1 males were easily recognizable when in the cage with WT littermates. Indeed, from P50 onwards, they constantly showed dull and ungroomed coat together with lesions along the tails. These lesions seem to be caused by compulsory-like behaviours. Spontaneous movements were found reduced in KI males for all

the testing periods. In accordance with the *Mecp2*-null mice, where the hind limb clasping appears after the reduction in the spontaneous movements (Cobolli Gigli et al., *paper under revision*), in Y120D males clasping appeared at around P67, delayed with respect to mobility impairments and to the same phenotype in the C57 strain.

The CD1 strain permitted the evaluation of tremor, which is usually linked to breathing abnormalities and which strongly affected our KI males since the first month of life.

Eventually, also these mutated animals are infertile.

A

| Males – P18 | total weight | brain |
|---|---|---|
| WT (gr) | 8,178 ± 0,255 | 0,373 ± 0,006 |
| KI (gr) | 5,722 ± 0,361 | 0,328 ± 0,008 |
| Reduction vs WT (%) | 30,03 | 12,16 |
| Significance | *** | ** |

B

| Males – P40 | total weight | brain | heart | kidney | gastrocnemius |
|---|---|---|---|---|---|
| WT (gr) | 27,400 ± 0,686 | 0,455 ± 0,012 | 0,185 ± 0,011 | 0,227 ± 0,012 | 0,132 ± 0,007 |
| KI (gr) | 23,806 ± 1,019 | 0,387 ± 0,008 | 0,138 ± 0,013 | 0,183 ± 0,011 | 0,113 ± 0,008 |
| Reduction vs WT (%) | 13,12 | 15,02 | 25,41 | 19,33 | 14,29 |
| Significance | * | *** | * | * | ns |

C

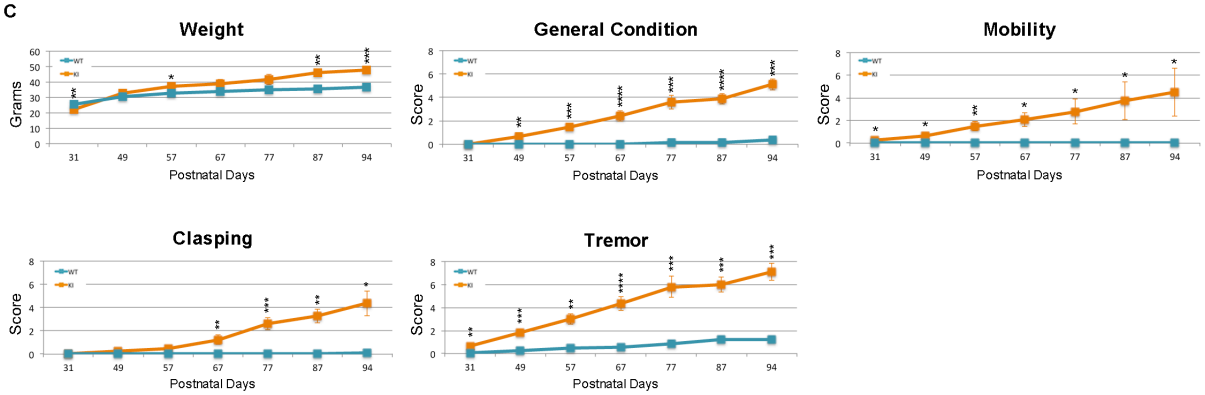


**Figure 8. Phenotypic characterization of the CD1 Y120D male mice.** A and B) Measures of the total body and organs weight of WT and KI males at P18 (A) at P40 (B) (n=4 to 8 and 6 to 11, respectively). Data are represented as mean±s.e.m. Tables also report the percentage of weight reduction calculated considering WT values as 100%. Significance is calculated with Student's *t* test (*p*-value: *<0.05; **<0.01; ***<0.001). C) Plot of total body weight and cumulative phenotypic score profiles of WT and KI male mice, showing the progression of RTT-like symptoms in the Y120D animals (n=7 WT and 6 KI at the beginning of the testing period). Data are represented as mean±s.e.m. Significance is calculated with Student's *t* test, which is performed on the pure (not cumulated) scores at each time point (*p*-value: *<0.05; **<0.01; ***<0.001; ****<0.0001).

Importantly, we had enough animals to perform the phenotypical characterization of CD1 heterozygous females. Since these mice were expected to be less symptomatic than the hemizygous males, they were evaluated every two weeks (Figure 9). Y120D KI females started to gain weight at around two/three months of age, becoming soon overweight with respect to WT controls. In the same time window, their general condition worsened and their coat was recognizable as it was less shiny and tidy. As expected, they were less symptomatic than males and they begun to show some slight mobility impairments and clasping behaviour

after 4 months of life. The most prominent phenotype was tremor that appeared already at P63.

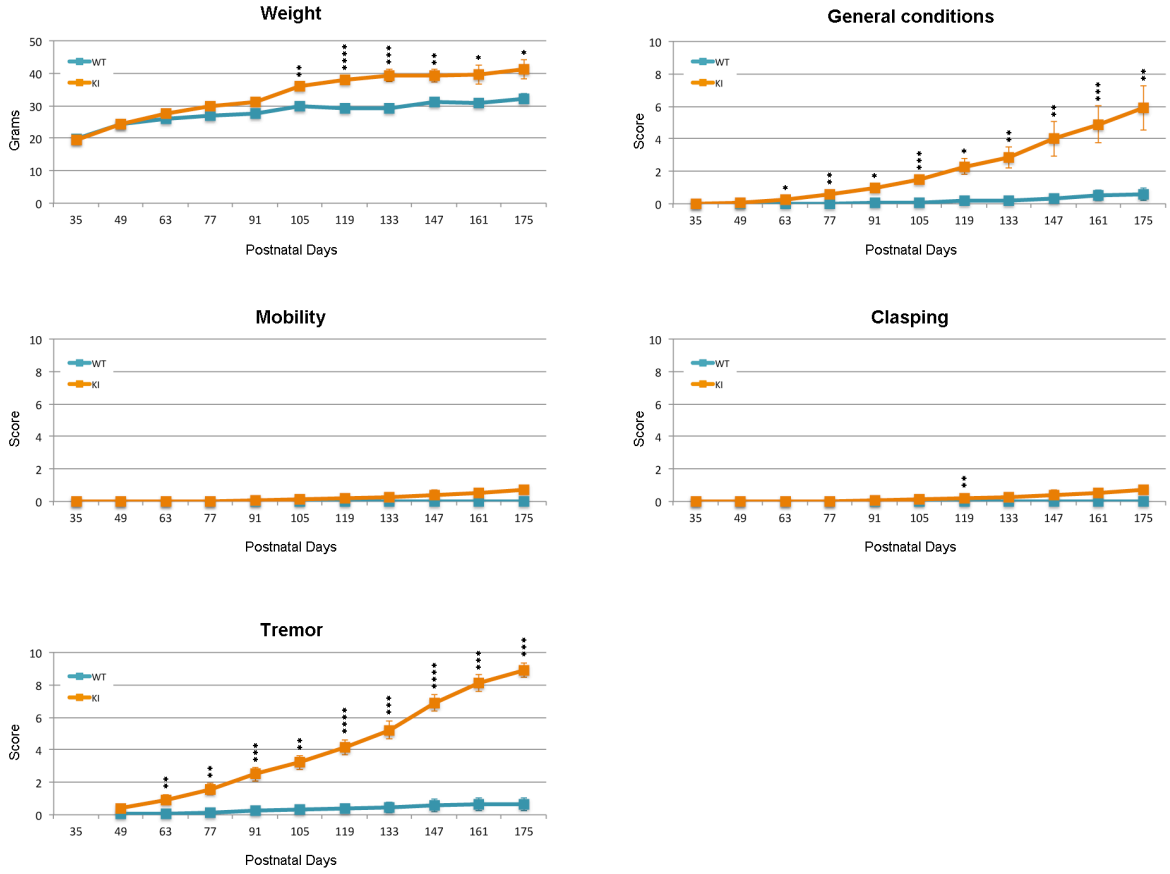


**Figure 9. Phenotypic characterization of the CD1 Y120D heterozygous female mice.** Plot of total body weight and cumulative phenotypic score profiles of WT and KI female mice, showing the progression of some RTT-like symptoms in the Y120D animals (n=8 WT and 7 KI at the beginning of the testing period). Data are represented as mean±s.e.m. Significance is calculated with Student's *t* test, which is performed on the pure (not cumulated) scores at each time point (*p*-value: *<0.05; **<0.01; ***<0.001; ****<0.0001).

*To conclude, we can state that the generated Mecp2 Tyr-120 mutation causes a host of gross phenotypical alterations that are displayed also by other RTT mouse models. These abnormalities are generally shared between two different genetic backgrounds and, as expected, are less severe in heterozygous females.*

## 3.3. Morphological alterations caused by the Y120D mutation

### *3.3.1. Cortical thickness and neuronal nuclear diameter in Y120D mouse*

We next sought to evaluate whether the pathogenic Y120D mutation of Mecp2 affects the overall morphology of neural tissues and cells, causing alterations that might be related to the development of the murine phenotypes.

Since it is well known that *Mecp2*-null mice show reduced cortical thickness (Kishi and Macklis, 2004), we exploited Nissl staining to compare cortical thickness in P30 WT and KI brains (Figure 10A). We measured the thickness of the frontal cortex, a brain area that has been previously involved in RTT pathogenesis (Kron et al., 2012). *Mecp2*$^{Y120D}$ hemizygous cortices do not show a dramatic reduction in thickness; a small reduction (≈5%) was only measured in the most rostral positions evaluated (Figure 10B, 1-3). Of note, the effect of Mecp2 loss on cortical thickness reported by Kishi and Macklis was approximately of the 10% and maintained throughout the different tested positions.

Another morphological feature that in our laboratory has been found altered in the absence of Mecp2 is the nuclear size of primary cultured neurons, which appears to be reduced as early as at DIV (days *in vitro*) 3 till DIV14, thus affecting neurons at different stages of maturation (Bedogni et al., 2015 *and unpublished data*). We analysed this parameter on differentiating WT and KI primary neurons at DIV7, by staining them with DAPI and an antibody directed against the neuronal marker TuJ1 (Figure 10C). We measured the nuclear sizes of TuJ1-positive cells using a dedicated software and we observed that nuclear diameter was unaffected in Y120D neurons (Figure 10 D,D',E).

*From these initial analyses we concluded that Tyr-120 mutation does not induce two main morphological defects usually linked to RTT, which therefore are not involved in the phenotype of the Y120D mice.* It remains to be determined whether other important features, such as dendritic branching and neuronal cell number, are altered or not in the KI situation and, thus, if they are causally related to the animals' symptomatology.

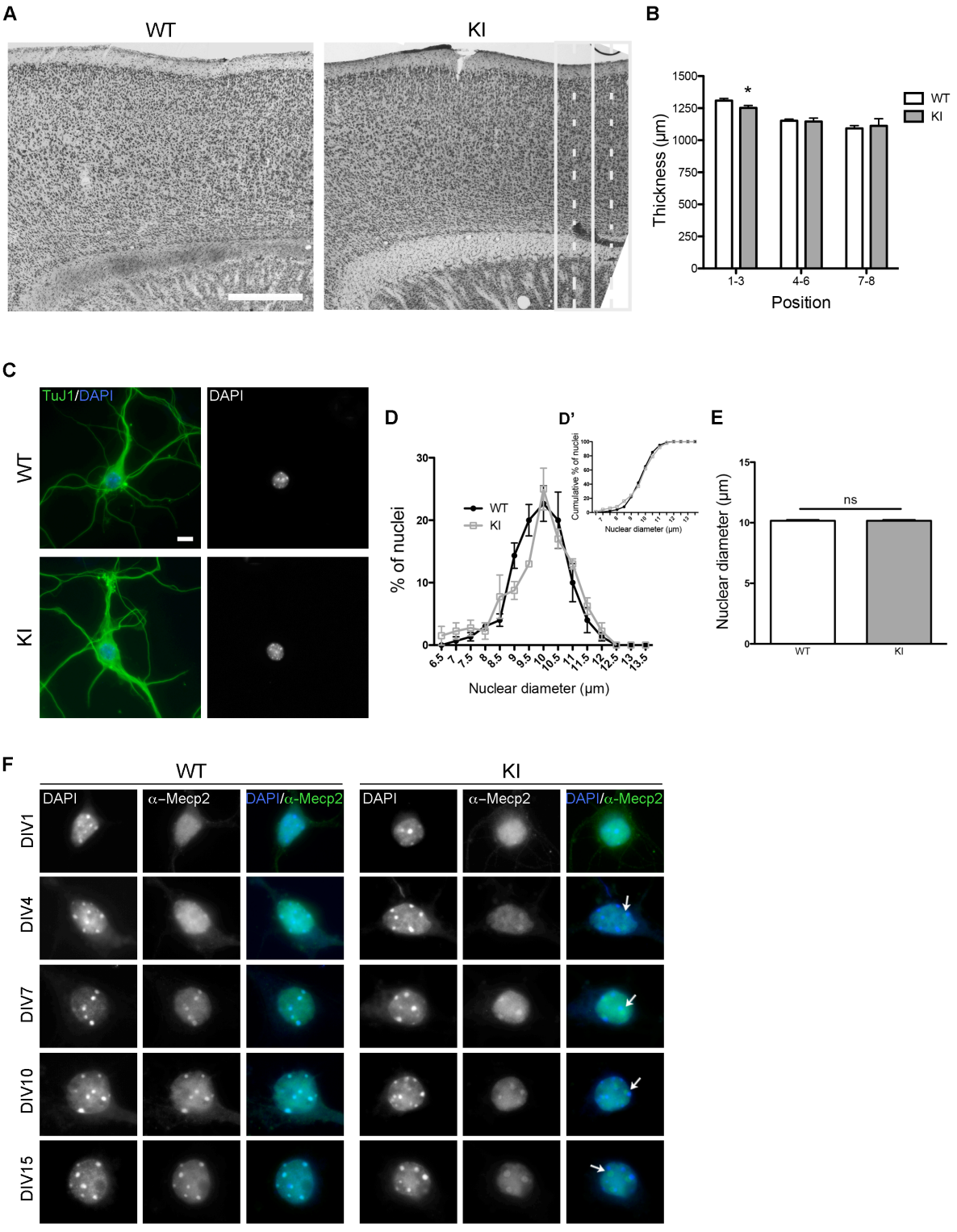


**Figure 10. Effects of the Y120D mutation on neural tissues/cells and on protein localization.** A) Nissl staining on sagittal brain slices of WT and KI mice at P30. On the KI image are exemplified two positions of the grid used to measure cortical thickness. Dashed lines indicate the middle of the columns/the points of measurement. Scale bar = 500 µm B) Quantification of the frontal cortex thickness in WT and KI males at P30 (n=4 WT and 5 KI). Thickness was evaluated in 8 different positions then mediated in 3 groups to minimize the experimental variability. Data are represented as mean±s.e.m. Significance is calculated with Student's *t* test (*p*-value: *=0.045). C) WT and KI cultured neurons, established from cortices at E17, immunostained at DIV7 for TuJ1/DAPI to specifically recognize neuronal

nuclei. Scale bar = 10 μm D and E) Morphological analyses of the WT and KI neuronal nuclear size (n=3 WT and 4 KI; at least 50 nuclei were measured for each animal). In D) is represented the size distribution of nuclei in %. Data are represented as mean±s.e.m. The cumulative analysis depicted in D') reveals no statistically significant difference between the WT and KI distributions of nuclear diameter. In E) is represented the mean nuclear diameter±s.e.m. Significance is calculated with Student's *t* test. F) Representative images of WT and KI cultured neurons, established from cortices at E17, immunostained at different DIV for Mecp2/DAPI. Images are taken at 100X magnification. The arrows on the merged images indicate the Mecp2-positive nuclear puncta found adjacent to chromocenters in the KI nuclei.

### *3.3.2. Mecp2 delocalization in Y120D neurons*

As already mentioned, in the nuclei of mouse cells Mecp2 predominantly associates with the pericentromeric heterochromatic regions through its binding to methylated DNA, giving rise to a peculiar staining with the protein both diffused throughout the nuclei and accumulated in discrete dots that colocalize with the heterochromatic foci (Nan et al., 1996).

Since the Y120D mutation occurs inside the methyl-DNA binding domain, we investigated whether the colocalization between Mecp2 and chromocenters was altered in mutated cultured neuronal cells (Figure 10F). As expected, we noticed that the wild-type protein, besides being diffused throughout the nucleus, forms foci that colocalize with the dots of DAPI as early as at DIV4. Interestingly, these foci – always colocalizing with chromocenters – appear more defined at DIV10 and DIV15, when neurons are more mature. Conversely, the mutated protein, while maintaining its diffuse distribution throughout the nuclei, fails to form foci colocalizing with the heterochromatic regions. Moreover, in the KI nuclei from DIV4 onwards we noticed the presence of Mecp2-positive nuclear puncta adjacent – but not overlapping – to the chromocenters. The identity of these structures remains to be determined. *The altered subnuclear distribution of the mutated protein suggests that the Tyr-120 residue substitution (and possibly also its phosphorylation) influences the affinity of Mecp2 for chromatin.* It is interesting to recall that all the other phosphorylation sites described so far, which are not found mutated in RTT patients, are not crucial for this aspect. Indeed, when they are mutated, the nuclear localization of Mecp2 is unaltered. On the contrary, the common pathogenic T158A and T158M mutations, which also occur in the MBD as Y120D, induce the mislocalization of the protein (Goffin et al., 2012; Lyst et al., 2013). *Altogether, these data suggest that the altered association between Mecp2 and heterochromatic regions might be a common consequence of the MBD mutations and might be involved in the pathogenic mechanisms leading to Rett syndrome.*

## 3.4. Biochemical alterations in the Y120D brains

To deepen our understanding of the KI mice phenotypes, we started to evaluate the consequences of the Y120D mutation from a molecular point of view.

### *3.4.1. The Y120D mutation affects the levels of Mecp2 and of its Ser-164 phospho-isoform in the central nervous system*

The precise regulation of the levels of MeCP2 is fundamental for the proper functioning of the central nervous system. Indeed, besides the described detrimental effects caused by *MECP2* loss-of-function mutations and decreased expression, also gene duplication and overexpression have pathogenic consequences, resulting in the so-called *MECP2* duplication syndrome (Chahrour and Zoghbi, 2007). Thus, we firstly investigated the effects of the Y120D substitution on Mecp2 protein expression in the cerebral tissues of adult and highly symptomatic C57BL6J males (at around P100). Via qPCR, we confirmed that – even at a late time point – the *Mecp2* mRNA transcription is not affected by the engineering of the genomic locus and by its point mutation (Figure 11A). Conversely, Western Blotting analysis showed that Mecp2 protein levels are significantly reduced (around 60/70%), with respect to the WT controls, both in cortices and hippocampi retrieved from KI mice (Figure 11B,C).
Since our unpublished data indicate that MeCP2 PTMs can change during development, we decided to confirm the reduction of Mecp2 protein levels in the CD1 Y120D hemizygous brains and to examine whether development might affect the amount of the pathogenic derivative of Mecp2, in which a phosphorylation site is altered (Figure 11D,E). To our surprise, we found that in the embryonic brains and in cortices harvested from newborn mice at P6 the protein expression was not affected by the Tyr-120 mutation, being unaltered between WT and KI samples. Conversely, Mecp2 levels appeared significantly decreased, with a 55/60% reduction with respect to the WT controls, in the Y120D cerebral cortices at P18 and at P40, when mice already display some behavioural anomalies, thus confirming the results obtained from C57BL6J KI. The data obtained at earlier time points demonstrated that the modification of the genomic locus is not *per se* detrimental for Mecp2 translation. Therefore, it is conceivable that the main reason of the observed diminished protein abundance is an increase in its degradative processes. Accordingly, preliminary *in vitro* experiments in which new protein translation has been inhibited through the administration of cycloheximide, allowing us to evaluate by WB the stability of Mecp2, suggest that the Y120D

mutation increases the rate of Mecp2 degradation, thus leading to its reduced levels (*data not shown*). Notably, this reduction in protein stability has also been described for the already mentioned T158A mutation (Goffin et al., 2012), highlighting a possible further common pathogenic consequence of these two *MECP2* alterations.

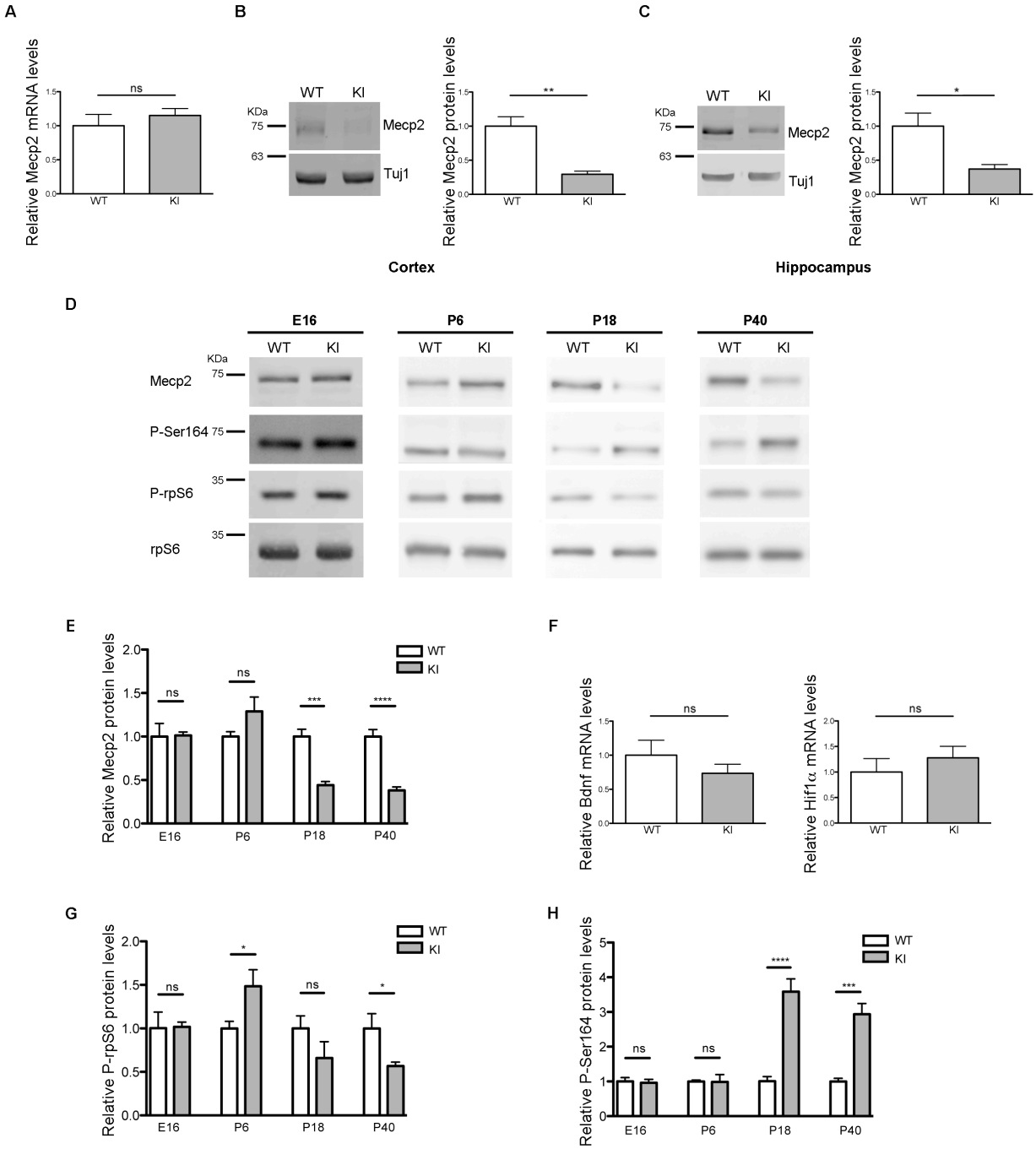


**Figure 11. Altered protein levels in adult C57 and in CD1 male mice.** A) *Mecp2* mRNA expression in the cortex of WT and KI C57 symptomatic male mice at around P100 (n=5 WT and 7 KI). Data are represented as mean±s.e.m. Significance is calculated with Student's *t* test. B) and C) Representative WB (*left*) and summary graphs (*right*) of Mecp2 protein levels in ≈P100 C57 WT and KI cortical (B) or hippocampal (C) lysates (n=4 WT and 5 KI cortices, 4

hippocampi for each genotype). TuJ1 was included as loading control. Data are represented as mean±s.e.m. Significance is calculated with Student's *t* test (*p*-value: *<0.05; **<0.01). D,E,G and H) Representative WB (D) and summary graphs (E,G,H) of Mecp2, P-rpS6 and P-Ser164 protein levels, assessed on E16 brains and P6, P18, P40 cortices harvested from WT and KI CD1 male mice (n=5 to 8 for each graphs). rpS6 was included as loading control. Data are represented as mean±s.e.m. Significance is calculated with Student's *t* test (*p*-value: *<0.05; ***<0.001; ****<0.0001). F) *Bdnf* and *Hif1α* mRNA expression in the cortex of WT and KI C57 symptomatic male mice at around P100 (n=5 WT and 6 KI for *Bdnf*, 5 WT and 7 KI for *Hif1α*). Data are represented as mean±s.e.m. Significance is calculated with Student's *t* test.

Another molecular analyses we performed was the evaluation of *Bdnf* and *Hif1α* transcription, since both downregulation of *Bdnf* and upregulation of *Hif1α* mRNA expression are two molecular defects commonly observed in *Mecp2*-null cerebral tissues (Chang et al., 2006; Fischer et al., 2009). Interestingly, in the cortices of symptomatic mutated males transcription of these mRNAs resulted unaltered with respect to the WT controls (Figure 11F).

Since a further alteration usually found associated with Mecp2 deficiency and often considered a marker of the disease progression is the reduction in the ribosomal protein S6 (rpS6) phosphorylation (Conti et al., 2015; Ricciardi et al., 2011), we evaluated whether the Tyr-120 mutation results in the same molecular defect. By Western Blotting analyses (Figure 11D,G) we observed that P-rpS6 is not reduced in KI cerebral tissues from the earlier time point till P18. However, rpS6 phosphorylation is significantly reduced in KI brains at P40, underscoring a possible impairment of translation in the mutated mice that could contribute to the development of the described RTT-like symptoms.

Nowadays, MeCP2 is often considered to be finely tuned by a sort of "regulatory code" placed by its many post-translational modifications and the existence of functional influences between the different PTMs has been postulated; however, no cross talks have been described so far. Considering that the aspartic acid substitution of Tyr-120 could possibly mimic a constitutively phosphorylation state, we wondered whether a cross talk between Tyr-120 phosphorylation and other PTMs does exist and whether Y120D mutation alters these putative interactions.

In our laboratory we are investigating the roles and the functional relevance of Mecp2 phosphorylation in another amino acid residue that is Ser-164. Recently, it has been observed that this brain-specific phospho-isoform (P-Ser164), whose PTM occurs right next to the MBD, is significantly enriched in the cerebral tissues of wild-type mice at P4, while its levels decrease during development, becoming significantly lower at P30 with respect to the early

postnatal period. Notably, when this residue is substituted with the non-phosphorylatable alanine, the mutated protein is more efficiently targeted to the heterochromatic foci than the WT one. On the contrary, when Serine-164 is mutated to aspartic acid, the S164D protein is more diffused into the nucleoplasm and less localized in chromocenters compared to both the WT and S164A constructs. To investigate whether a cross talk between Ser-164 and Tyr-120 modifications does exist, we evaluated the abundance of the P-Ser164 isoform of Mecp2 in WT and KI cerebral tissues at different time points (Figure 11D,H). We noticed that in the embryonic and early postnatal periods Ser-164 phosphorylation is unaltered between the two genotypes. Differently, at P18 and at P40 this amino acid residue is significantly hyper-phosphorylated in the KI cortices, leading us to hypothesize the existence of a molecular association between the Tyrosine-120 phosphorylation/mutation and the Serine-164 post-translational modification. The nature of this cross talk and its spatiotemporal features still remain to be dissected.

### *3.4.2. The Y120D mutation decreases the affinity of Mecp2 for DNA*

The study of the Ser-164 phosphorylation carried out in our laboratory has revealed that this phospho-isoform corresponds to a fraction of Mecp2 that binds chromatin weakly. Indeed, in brains of adult wild-type mice, it appears to be more soluble than the total protein and at P4, when a greater portion of Mecp2 is modified on this residue, the solubility of the total methyl-binding protein is enhanced. Moreover, also the mutant S164D construct *in vitro* results more soluble than the WT one. Considering that the Tyr-120 mutation occurs inside the MBD of Mecp2 and that the mutated protein has an altered subnuclear colocalization with the heterochromatic foci, we wondered whether – similarly to the Ser-164 PTM – the pathogenic substitution of this amino acid residue could alter the affinity of Mecp2 for chromatin. Thus, we performed a salt extraction assay (Figure 12A) on brains of WT and KI adult mice (P40) and we noticed that, compared to the WT one, the mutated protein requires a lower concentration of NaCl salt to be extracted from DNA: indeed, the peak of detachment for the WT Mecp2 is at around 600 mM NaCl, whereas for the Y120D protein it is at around 500 mM NaCl, underscoring the increased solubility of the mutated Mecp2. By evaluating the salt extraction of the P-Ser164 isoform from DNA in the same WT and KI brain extracts (Figure 12B), we observed that also this phospho-isoform appears more soluble in the Y120D samples, with a slight shift of the curve of detachment towards lower NaCl concentrations. This result suggests that the increased solubility of the total Mecp2 found in KI tissues is not

only ascribable to the Ser-164 hyper-phosphorylation described in Y120D cortices (Figure 11E); instead, it is possible to hypothesize that Ser-164 and Tyr-120 modifications exert an – at least – additive effect both influencing the DNA binding properties of Mecp2.

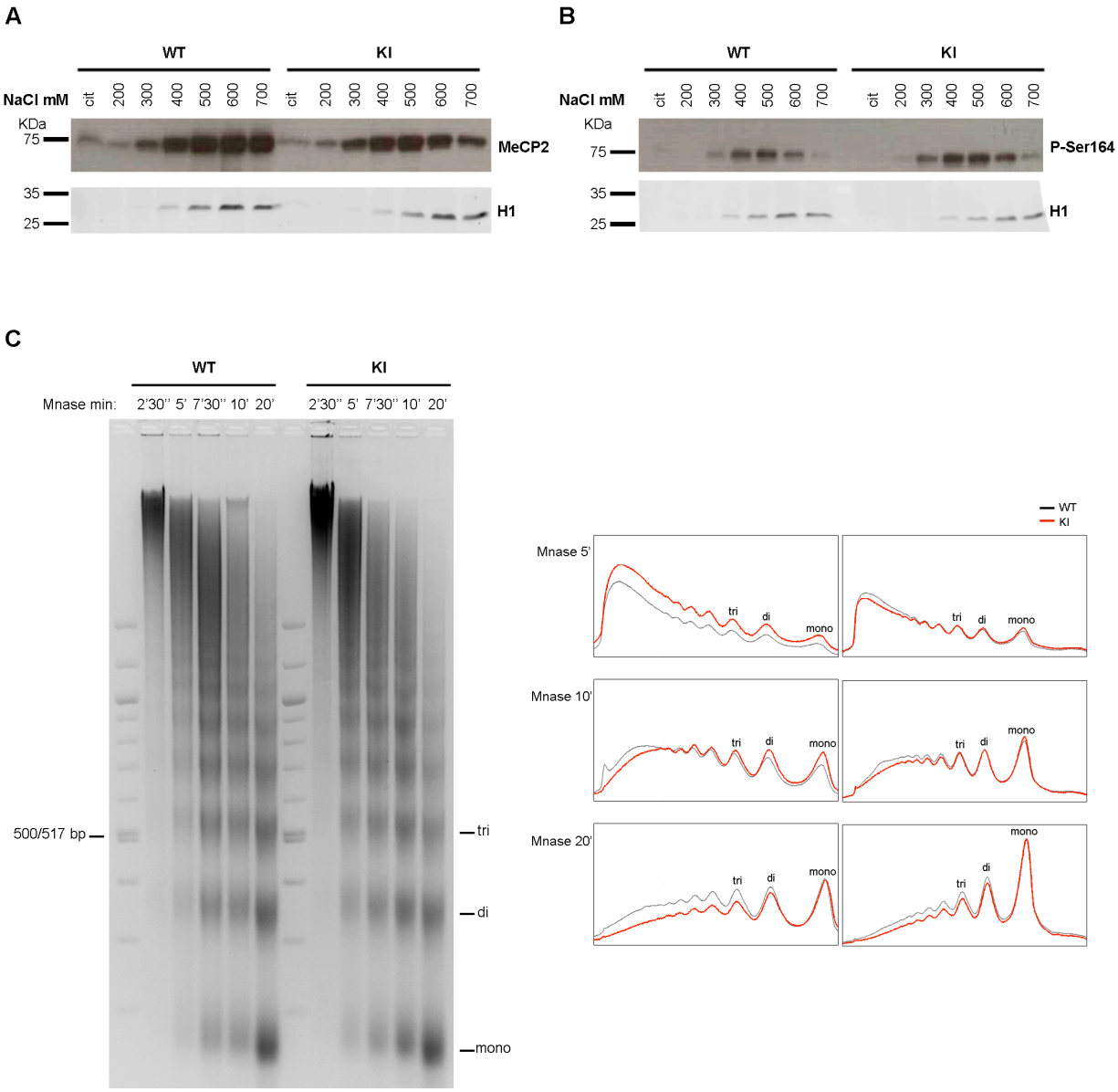


**Figure 12. Y120D mutation alters the DNA binding properties of Mecp2 and chromatin compaction.** A and B) WB showing salt extraction of WT Mecp2 and Y120D mutated Mecp2 (A) or their P-Ser164 phospho-isoform (B) with increasing concentrations of NaCl, from brains of WT and KI P40 CD1 males (n=3). H1 was included as control of the salt extraction procedures. C) 2% agarose gel (*left*) and densitometry plots (*right*) showing the progressive generation of DNA fragments at different time points of MNase digestion of brain nuclei isolated from WT and KI CD1 males (n=3). Tri-, di- and mono-nucleosome are underlined. Densitometry plots refer to the represented agarose gel and to a second replicative experiment.

To investigate the effect of the Y120D mutation on the role of Mecp2 as a chromatin factor, we evaluated chromatin accessibility by performing a time-course of micrococcal nuclease

(MNase) digestion on the cerebral nuclei isolated from WT and KI mice at P40. The release of the different species of nucleosome (such as the tri-, di-, mono-nucleosome) from the digested DNA was visualized on a 2% agarose gel (Figure 12C, *left panel*) and, then, on densitometry plots (Figure 12C, *right panels*). Through the analysis of these plots we noticed that, at the different time points of MNase incubation, the DNA obtained from KI nuclei seems to be more efficiently digested into the smallest nucleosome species, in particular into the mono-nucleosome. Thus, when the Mecp2 Tyr-120 residue is mutated to aspartic acid, chromatin appears more accessible.

*In conclusion, these data suggest that, in adult brains, the MBD Y120D mutation alters MeCP2 affinity for chromatin and/or methylated DNA and affects the regulation of global chromatin architecture. This could possibly lead to transcriptional impairments, ultimately contributing to the development of the phenotypes observed in the KI mice.*

# 4. Discussion

Over the last decades, great efforts have been made to understand the pathogenic mechanisms of Rett syndrome and the biological functions of MeCP2, whose mutations are the primary cause of this neurological disease (Amir et al., 1999). Despite the vast interest in these arguments and the hard work put on RTT research, our comprehension of MeCP2 features is still far from being complete. The original idea of MeCP2 as a gene-specific transcriptional repressor that binds methyl-CpG DNA has been replaced by a view in which the protein is genome-wide bound, tracking methyl-CpG density and acting as an histone-like component of the chromatin (Skene et al., 2010). This concept has been further complicated by the findings that MeCP2 is able to bind also unmethylated DNA (Ghosh et al., 2010b), 5-hydroxymethylcytosine molecules (Mellen et al., 2012) and methylated cytosines not belonging to a CpG dinucleotide (Chen et al., 2015). Moreover, MeCP2 appears to be characterized by a great multifunctionality, acting also as a transcriptional activator (Chahrour et al., 2008), being involved in alternative splicing and protein translation regulation (Long et al., 2011; Young et al., 2005) and, as newly indicated in our laboratory, contributing to the centrosomal functions (Bergo et al., 2015). All these findings are still debated in the RTT field and some important aspects, such as the spatiotemporal regulation of MeCP2 roles, need to be clarified. Importantly, in the last years new evidences have suggested that this protein multifunctionality could be allowed and regulated by its intrinsically disorganized structure and by its post-translational modifications. These two biological features could influence both the DNA binding properties of MeCP2 and its interactions with functional partners, therefore, finely tuning its functions (Bedogni et al., 2014; Bellini et al., 2014). Consequently, a number of new mouse models carrying mutations on PTM sites have been generated in order to understand the importance of specific modifications of MeCP2. In this context, we found interesting to study Tyr-120 phosphorylation (Dephoure et al., 2008) because – differently to all the other PTMs modelled so far – its mutation into aspartic acid was associated with Rett syndrome (Inui et al., 2001). Unfortunately, we lack updated clinical data regarding the disease course of this RTT patient, which could have given us some hints on the functional relevance of this residue. However, considering that this site is highly conserved in mammals and that its pathogenic substitution to aspartic acid possibly mimics a constitutively phosphorylated state, we hypothesized that the dynamic modification of Tyr-120 is required for proper functioning of MeCP2. At first, this phospho-isoform was characterized *in vitro,* permitting to demonstrate that at least a fraction of the Y120(P) isoform of MeCP2 is

localized at the centrosome both in dividing cells and in post-mitotic neurons. Importantly, the lack of MeCP2 is associated to several centrosomal-related phenotypes, including proliferation defects that cannot be rescued by the Y120D protein derivative, suggesting that the phospho-Y120 isoform influences cell proliferation (Bergo et al., 2015). To better characterize the functional relevance of the Tyr-120 residue and of its post-translational modification, we generated a KI mouse model carrying the Mecp2 Y120D pathogenic substitution. We found this animal model, reproducing a human missense mutation, useful for a better comprehension of RTT pathogenic mechanisms. Indeed, although only few girls are affected by large deletion of *MECP2*, *Mecp2*-null mice are the most commonly used models in Rett syndrome research (Ricceri et al., 2008). The complete absence of the methyl-binding protein together with the associated severe phenotypes probably leads to compensatory mechanisms in these animals, that might mask the real mechanisms lying beneath the disease development, leading scientists to focus on the wrong therapeutic targets. We, therefore, firmly believe that our new Y120D mouse model, together with other KI mice mimicking patients' mutations, could be useful for unravelling specific aspects of RTT development.

In this study we present an initial characterization of our novel *Mecp2*$^{Y120D}$ line aimed at identifying overt mouse phenotypes as well as cellular and molecular defects caused by the pathogenic mutation; studies were performed in two different genetic backgrounds. The C57BL6J is the most commonly used strain in RTT research. However, the maintenance of *Mecp2*-null C57 colonies presents a lot of drawbacks, rendering quite difficult to obtain the number of animals necessary to run statistically significant experiments. Importantly, also the Y120D C57 line showed problems such as the generation of small litters, episodes of cannibalism and a low number of successful pregnancies. Thus, we transferred the Y120D mutated allele in the CD1 background. Indeed, the CD1 *Mecp2*-null animals were previously demonstrated to be more robust than the C57 one, while still recapitulating the typical defects caused by the gene depletion (Cobolli Gigli et al., *paper under revision*; Bedogni et al., 2015). As expected, maintenance of the Y120D CD1 line resulted dramatically less complicated. The characterization of the C57 and CD1 mutated mice revealed only few and slight phenotypic differences, therefore, indicating that the CD1 background is suitable for the study of the Mecp2 Tyr-120 mutation.

The first gross phenotypical abnormality that we observed in our new mouse model was the alteration of mice weight: C57 KI males appeared smaller than their WT controls, while C57 heterozygous females and CD1 KI males and females resulted strongly overweight in

adulthood. As for the *Mecp2*-null model (Ricceri et al., 2008; Samaco et al., 2013), the observed altered weights clearly appear to be influenced by the animal genetic backgrounds. However, this phenotype could be related to metabolic impairments already described in RTT patients and in *Mecp2*-depleted mice of different strains, affecting – for example – cholesterol homeostasis and leptin signalling (Blardi et al., 2009; Buchovecky et al., 2013; Park et al., 2014). Considering the localization of the Y120(P) phospho-isoform at centrosomes, it is tempting to speculate that the strong weight alteration seen in KI mice could also rely on the MeCP2 centrosomal functions. Indeed, it is known that this organelle is fundamental for the biogenesis of the primary cilium, a sensing and signalling structure located on the surface of virtually all cell types. Further, an on-going parallel research of our laboratory has collected a bunch of data demonstrating that Mecp2 deficiency severely affects primary cilium formation *in vitro* and *in vivo* (Bergo et al., *manuscript in preparation*). Interestingly, primary cilium is involved in a group of severe genetic disorders generally called ciliopathies often characterized by the tendency of patients and mouse models to become obese (Berbari et al., 2013).

Exploiting an already published scoring system (Guy et al., 2007 and several subsequent publications), we observed that Y120D male mice manifest gross RTT-like phenotypes that have been reported also in the *Mecp2*-null mouse models, such as poor general conditions, reduced spontaneous movements, hind limb clasping and tremors. Interestingly, in our KI line the development of RTT symptoms is associated with the reduction of rpS6 phosphorylation in brains, which is often regarded as a possible biomarker of disease progression in *Mecp2*-null mice (Ricciardi et al., 2011). The time window in which symptoms appear and develop is quite similar between Y120D and null hemizygous males. However, the expected lifespan of the KI mice (approximately 15 weeks) is longer than that of the *Mecp2*$^{-/y}$ animals (around 10 weeks of age) (Cobolli Gigli et al., *paper under revision*; Guy et al., 2001). Consistently with the heterozygous expression of the mutated allele, Y120D females appear less symptomatic than KI males and have an increased lifespan. We plan to complete the herein presented phenotypical characterization from different points of view. Indeed, in collaboration with the laboratory of prof. D'Adamo at the San Raffaele Scientific Institute of Milan, we are performing a battery of behavioural tests on WT and KI animals to precisely assess whether the Y120D mice suffer from specific locomotor deficits, from impairments in their learning and memory ability or from anxiety-related behaviours. Moreover, we are planning EEG recordings to analyze whether the mutation of Tyr-120 results in seizures and epilepsy, two common and harsh symptoms affecting RTT patients. Even if our phenotypical

characterization is still incomplete and partially differs from that of other mouse models of *Mecp2* functions, we highlight that the Y120D model is affected by more severe impairments with respect to the *MeCP2*$^{S421A}$ and *Mecp2*$^{S421A/S424A}$ mice, which have normal lifespan and only few behavioural alterations (Cohen et al., 2011; Li et al., 2011). Conversely, the symptomatology of our new KI mouse model appears similar to that of the T158A mice (Goffin et al., 2012). While no patients with S421 or S424 alterations have been reported so far, T158 is one of the most commonly mutated sites in Rett syndrome. Apart from underlining the major relevance of some residues of MeCP2, these observations appear to reinforce the validity of using mouse models for the study of RTT pathogenic mechanisms.

*Mecp2*-null brains are characterized by some morphological alterations such as reduced thickness of the neocortex, reduced neuronal nuclear and soma size and defective dendritic branching (Bedogni et al., 2015; Belichenko et al., 2009; Kishi and Macklis, 2004); therefore, we found it relevant to analyze the influence of Y120D mutation on these aspects. We noticed that neuronal nuclear size is unaffected by the Y120D derivative. Moreover, we observed that thickness of the frontal cortex is only marginally decreased in the KI adult males: this slight reduction might not be of relevance for the general bad condition of the novel mouse line, thus we can anticipate that we are not considering further studies on this aspect. To assess whether the Y120D substitution induces any other morphological alteration possibly involved in the development of RTT-like phenotypes we will measure the soma size and the density of KI neurons, together with the extent of their dendritic branching.

Molecularly, we demonstrated that the Y120D mutation does not affect the methyl-binding protein levels in the embryonic and early post-natal brains; however, cerebral Mecp2 levels appear significantly decreased in KI males at around P20 and this reduction is maintained during adulthood both in C57 and in CD1 animals. Moreover, we also showed that in adult brains the mutated protein is characterized by an increased solubility with respect to the WT one, a finding that underlies a reduced affinity for DNA. Accordingly, the subnuclear distribution of Y120D Mecp2 is altered in cultured neurons, with the protein failing to colocalize with the highly methylated pericentromeric heterochromatic foci. Of interest, the molecular phenotypes described in adult brain are analogous to those observed when Mecp2 is mutated in its Thr-158 residue (Goffin et al., 2012), thus possibly linking missense mutations occurring in the MBD to same or at least similar pathogenic mechanisms.

Notably, in WT neurons the Mecp2/chromocenters colocalization begins to appear at around DIV4, while at DIV1 Mecp2 foci are not evident and wild-type and mutated protein are similarly diffused in the nuclei. This observation is in accordance with previous *in vivo* results showing that the subnuclear distribution of wild-type Mecp2 changes through time, passing from a diffuse to a punctate staining with the development of mouse brain and with the related increase in protein levels (Shahbazian et al., 2002b). However, it is important to note that the defective cellular localization of the mutated Mecp2 is not a consequence of its reduced levels. Indeed, a decreased affinity of the protein for chromocenters appears evident also when the Y120D derivative construct is over-expressed in cultured cells (Agarwal et al., 2011; Kudo et al., 2003). It would be important to determine whether the diminished binding of the mutated protein to DNA is caused by a reduced affinity of Y120D Mecp2 for methylated DNA in general or specifically for methylated-CpG, 5-hydroxymethylcytosine or for methylated cytosines not belonging to a CpG dinucleotide. Indeed, other substitutions of a single residue in the MBD, such as R133C, have already been described as preferentially impacting the binding of MeCP2 to a specific substrate. This raised the possibility that also post-translational modifications could finely regulate the specificity of MeCP2/DNA association (Mellen et al., 2012). Thus, dissecting this aspect in our KI model, in which a constitutively Y120(P) state is mimicked, could help understanding both the mechanisms leading to RTT when this residue is mutated and the physiological impact of the dynamic Tyr-120 phosphorylation on the MeCP2 binding properties.

The observed reduced levels of the mutated protein in mature brains are probably ascribable to an augment in its degradation. Even if it is certainly conceivable that the Tyr-120 alteration might affect some motifs involved in proteolytic degradation or in protein ubiquitination, considering the altered subnuclear localization of the Y120D derivative we prefer to hypothesize a model in which the MBD mutation reduces the protein affinity for DNA or chromatin, therefore causing an increase in MeCP2 solubility and the consequent degradation of the unbound protein. In this context, a fundamental question is why Y120D Mecp2 levels are reduced only after the early post-natal period. A possible and suggestive answer is that early in life, when the central nervous system is more immature, MeCP2 is highly phosphorylated in its Tyrosine-120 residue (or in other MBD sites), and this physiologically reduces the affinity of MeCP2 for DNA. Unfortunately, the lack of a good antibody recognizing the Y120(P) isoform prevents us to confirm this hypothesis, which is however supported by the diffuse MeCP2 staining in immature neurons and by our unpublished results demonstrating that in WT brains at P4 chromatin is more accessible than in adulthood. If this

model is correct, at early time points the WT and mutated proteins should have a quite similar behaviour and the initial presence of a protein constitutively phosphorylated on its Tyr-120 site should not be – strongly – deleterious for the cells, which thus do not degrade it. Accordingly, we expect the mutated and wild-type protein to have similar solubility in the developing brain: a possibility that we will test in the next future. As a consequence of this theory, we could hypothesize that our KI mouse model does not suffer from embryonic developmental defects, which could justify why its cortical thickness is not strongly impaired, differently from what seen in the null models (Kishi and Macklis, 2004). The Y120D mouse, thus, could appear as an interesting and useful model to understand the consequences of post-natal reduced Mecp2 functionality (without the influence of embryonic effects) and it could help dissecting the functional roles of Mecp2 during different life periods (the embryonic/early post-natal and the post-natal/adult ones). Indeed, we hypothesize that the methyl-binding protein exerts different functions in different time-windows, therefore changing its biochemical properties throughout time, possibly thanks to different post-translational modifications. A detailed analysis of these aspects could help RTT researchers to understand whether pathogenic human mutations induce different phenotypes depending on when they alter MeCP2 functioning.

Even if all this view is attractive, in the context of the Y120D mutation, it could be complicated by two important factors. First, we have to consider that – as already mentioned – the Y120(P) phospho-isoform localizes at centrosomes in both dividing and post-mitotic cells and that it is involved in the MeCP2 centrosomal functions. Notably, when Tyrosine-120 is mutated to aspartic acid cells suffer from proliferation defects and the protein has an altered affinity for the organelle (Bergo et al., 2015 *and unpublished results*). It is therefore conceivable that the developing brains could be affected by centrosomal alterations, that might influence neural progenitors and glial cells proliferation, neuronal differentiation and/or primary cilia formation and functioning (Higginbotham and Gleeson, 2007; Kim and Dynlacht, 2013). The second factor that we have to consider is that, being Mecp2 "constitutively phosphorylated", the dynamic regulation of its Tyr-120 PTM could result altered even at early time points. This could temporarily affect its binding to DNA and thus induce transcriptional defects. In other words, it is possible that our KI mice suffer from subtle impairments already during embryogenesis and early post-natal periods. To evaluate if this is true, in accordance with a recent publication we will evaluate the responsiveness of developing *Mecp2*$^{Y120D}$ neurons to external stimuli; further we will assess in *Mecp2*$^{Y120D}$ embryonic and perinatal cerebral tissues the transcription levels of genes already found

deregulated in the *Mecp2*-null embryonic cortices (Bedogni et al., 2015). Eventually, we will phenotypically characterize KI and WT animals in their first weeks after birth, evaluating whether evident neurological symptoms are already present in newborn mice.

For what concerns the late post-natal periods, we believe that RTT-like phenotypes could be caused by the alteration in the DNA binding properties of the Y120D derivative that we described in mature brains, which likely results in impaired gene transcription. Moreover, since MeCP2 levels are tightly regulated in the central nervous system and even slight perturbations of its expression result in neurological phenotypes (Chahrour and Zoghbi, 2007), it is probable that the observed reduction in protein abundance also contributes to the disease pathogenesis in adulthood.

Our results showed that in KI adult brains chromatin is more accessible to MNase digestion with respect to the WT controls. This structural defect could be either a consequence of the Y120D altered affinity for DNA or a secondary effect of the decreased protein abundance. In any case, it is reasonable that by influencing gene expression this alteration represents a further contribution to the development of RTT-like phenotypes. In this context, it will be interesting to determine the accessibility of neuronal chromatin of KI embryos and young animals, in order to confirm (or not) an equal behaviour of the WT and mutated protein at early time points.

Although less probable because of the MBD localization of Y120, in the future we will also analyse whether the studied mutation influences the interaction of MeCP2 with relevant molecular partners, such as the corepressor complex N-CoR and ATRX (Kokura et al., 2001; Nan et al., 2007).

Eventually, considering that a cross talk between MeCP2 PTMs has been postulated, we evaluated the influence of the Y120D mutation on the phosphorylation of Ser-164, a residue under investigation in our laboratory. The modification of this site is enriched during the early post-natal period and appears to increase the solubility of total MeCP2. Moreover, similarly to what seen for the Y120D derivative, when Ser-164 is mutated to an aspartic acid, the affinity of the protein for chromocenters is reduced (Stefanelli et al, *manuscript in preparation*). Notably, we observed that from P18 onwards the amount of P-Ser164 is significantly increased in KI brains, demonstrating that Tyr-120 mutation (and possibly its phosphorylation) somehow induces the modification of this second residue, which could – at least in part – mediate some of the Y120D phenotypic consequences. However, it is important to observe that so far no patient mutated in S164 has been described. Why, in our KI model,

the phosphorylation of Ser164 is enriched only in adulthood? A possible answer to this question is that, at early time points, almost all the molecules of MeCP2 are already phosphorylated on this site. This scenario might well fit with our previous hypothesis of a great abundance of Y120(P) in the embryonic and peri-natal life and with the idea of a cross talk between the two PTMs. In the future we will also try to determine whether the Tyr-120 mutation induces other post-translational modifications that could influence the protein activities.

In conclusion, the KI mouse model herein reported is characterized by an extremely complex molecular phenotype. Decreased Mecp2 abundance, reduced protein affinity for DNA/chromatin, altered chromatin compaction and impaired interactions with post-translational modifications and binding partners could all participate to the pathogenic mechanisms leading to the development of RTT-like symptoms. Altogether these defects could affect gene transcription regulation, with different severity depending on the analysed time-window: this is an important aspect that we propose to evaluate in the next future. Finally, as mentioned, another fundamental aspect that has to be studied in depth is whether altered centrosomal activities of the mutated protein could contribute to the disease development.

# 5. Bibliography


Adams, V.H., S.J. McBryant, P.A. Wade, C.L. Woodcock, and J.C. Hansen. 2007. Intrinsic disorder and autonomous domain function in the multifunctional nuclear protein, MeCP2. *J Biol Chem*. 282:15057-64.

Agarwal, N., T. Hardt, A. Brero, D. Nowak, U. Rothbauer, A. Becker, H. Leonhardt, and M.C. Cardoso. 2007. MeCP2 interacts with HP1 and modulates its heterochromatin association during myogenic differentiation. *Nucleic Acids Res*. 35:5402-8.

Agarwal, N., A. Becker, K.L. Jost, S. Haase, B.K. Thakur, A. Brero, T. Hardt, S. Kudo, H. Leonhardt, and M.C. Cardoso. 2011. MeCP2 Rett mutations affect large scale chromatin organization. *Hum Mol Genet*. 20:4187-95.

Alvarez-Saavedra, M., L. Carrasco, S. Sura-Trueba, V. Demarchi Aiello, K. Walz, J.X. Neto, and J.I. Young. 2010. Elevated expression of MeCP2 in cardiac and skeletal tissues is detrimental for normal development. *Hum Mol Genet*. 19:2177-90.

Amir, R.E., I.B. Van den Veyver, M. Wan, C.Q. Tran, U. Francke, and H.Y. Zoghbi. 1999. Rett syndrome is caused by mutations in X-linked MECP2, encoding methyl-CpG-binding protein 2. *Nat Genet*. 23:185-8.

Ariani, F., G. Hayek, D. Rondinella, R. Artuso, M.A. Mencarelli, A. Spanhol-Rosseto, M. Pollazzon, S. Buoni, O. Spiga, S. Ricciardi, I. Meloni, I. Longo, F. Mari, V. Broccoli, M. Zappella, and A. Renieri. 2008. FOXG1 is responsible for the congenital variant of Rett syndrome. *Am J Hum Genet*. 83:89-93.

Armstrong, D.D. 2005. Neuropathology of Rett syndrome. *J Child Neurol*. 20:747-53.

Ballas, N., D.T. Lioy, C. Grunseich, and G. Mandel. 2009. Non-cell autonomous influence of MeCP2-deficient glia on neuronal dendritic morphology. *Nat Neurosci*. 12:311-7.

Bedogni, F., C. Cobolli Gigli, D. Pozzi, R.L. Rossi, L. Scaramuzza, G. Rossetti, M. Pagani, C. Kilstrup-Nielsen, M. Matteoli, and N. Landsberger. 2015. Defects During Mecp2 Null Embryonic Cortex Development Precede the Onset of Overt Neurological Symptoms. *Cereb Cortex*.

Bedogni, F., R.L. Rossi, F. Galli, C. Cobolli Gigli, A. Gandaglia, C. Kilstrup-Nielsen, and N. Landsberger. 2014. Rett syndrome and the urge of novel approaches to study MeCP2 functions and mechanisms of action. *Neurosci Biobehav Rev*. 46 Pt 2:187-201.

Belichenko, P.V., A. Oldfors, B. Hagberg, and A. Dahlstrom. 1994. Rett syndrome: 3-D confocal microscopy of cortical pyramidal dendrites and afferents. *Neuroreport*. 5:1509-13.

Belichenko, P.V., E.E. Wright, N.P. Belichenko, E. Masliah, H.H. Li, W.C. Mobley, and U. Francke. 2009. Widespread changes in dendritic and axonal morphology in Mecp2-mutant mouse models of Rett syndrome: evidence for disruption of neuronal networks. *J Comp Neurol*. 514:240-58.

Bellini, E., G. Pavesi, I. Barbiero, A. Bergo, C. Chandola, M.S. Nawaz, L. Rusconi, G. Stefanelli, M. Strollo, M.M. Valente, C. Kilstrup-Nielsen, and N. Landsberger. 2014. MeCP2 post-translational modifications: a mechanism to control its involvement in synaptic plasticity and homeostasis? *Front Cell Neurosci*. 8:236.

Berbari, N.F., R.C. Pasek, E.B. Malarkey, S.M. Yazdi, A.D. McNair, W.R. Lewis, T.R. Nagy, R.A. Kesterson, and B.K. Yoder. 2013. Leptin resistance is a secondary consequence of the obesity in ciliopathy mutant mice. *Proc Natl Acad Sci U S A*. 110:7796-801.

Bergo, A., M. Strollo, M. Gai, I. Barbiero, G. Stefanelli, S. Sertic, C. Cobolli Gigli, F. Di Cunto, C. Kilstrup-Nielsen, and N. Landsberger. 2015. Methyl-CpG binding protein 2 (MeCP2) localizes at the centrosome and is required for proper mitotic spindle organization. *J Biol Chem*. 290:3223-37.

Blardi, P., A. de Lalla, T. D'Ambrogio, G. Vonella, L. Ceccatelli, A. Auteri, and J. Hayek. 2009. Long-term plasma levels of leptin and adiponectin in Rett syndrome. *Clin Endocrinol (Oxf)*. 70:706-9.

Buchovecky, C.M., S.D. Turley, H.M. Brown, S.M. Kyle, J.G. McDonald, B. Liu, A.A. Pieper, W. Huang, D.M. Katz, D.W. Russell, J. Shendure, and M.J. Justice. 2013. A suppressor screen in Mecp2 mutant mice implicates cholesterol metabolism in Rett syndrome. *Nat Genet*. 45:1013-20.

Carro, S., A. Bergo, M. Mengoni, A. Bachi, G. Badaracco, C. Kilstrup-Nielsen, and N. Landsberger. 2004. A novel protein, Xenopus p20, influences the stability of MeCP2 through direct interaction. *J Biol Chem*. 279:25623-31.

Chahrour, M., S.Y. Jung, C. Shaw, X. Zhou, S.T. Wong, J. Qin, and H.Y. Zoghbi. 2008. MeCP2, a key contributor to neurological disease, activates and represses transcription. *Science*. 320:1224-9.

Chahrour, M., and H.Y. Zoghbi. 2007. The story of Rett syndrome: from clinic to neurobiology. *Neuron*. 56:422-37.

Chang, Q., G. Khare, V. Dani, S. Nelson, and R. Jaenisch. 2006. The disease progression of Mecp2 mutant mice is affected by the level of BDNF expression. *Neuron*. 49:341-8.

Chen, L., K. Chen, L.A. Lavery, S.A. Baker, C.A. Shaw, W. Li, and H.Y. Zoghbi. 2015. MeCP2 binds to non-CG methylated DNA as neurons mature, influencing

transcription and the timing of onset for Rett syndrome. *Proc Natl Acad Sci U S A*. 112:5509-14.

Chen, R.Z., S. Akbarian, M. Tudor, and R. Jaenisch. 2001. Deficiency of methyl-CpG binding protein-2 in CNS neurons results in a Rett-like phenotype in mice. *Nat Genet*. 27:327-31.

Chen, W.G., Q. Chang, Y. Lin, A. Meissner, A.E. West, E.C. Griffith, R. Jaenisch, and M.E. Greenberg. 2003. Derepression of BDNF transcription involves calcium-dependent phosphorylation of MeCP2. *Science*. 302:885-9.

Cohen, S., H.W. Gabel, M. Hemberg, A.N. Hutchinson, L.A. Sadacca, D.H. Ebert, D.A. Harmin, R.S. Greenberg, V.K. Verdine, Z. Zhou, W.C. Wetsel, A.E. West, and M.E. Greenberg. 2011. Genome-wide activity-dependent MeCP2 phosphorylation regulates nervous system development and function. *Neuron*. 72:72-85.

Conti, V., A. Gandaglia, F. Galli, M. Tirone, E. Bellini, L. Campana, C. Kilstrup-Nielsen, P. Rovere-Querini, S. Brunelli, and N. Landsberger. 2015. MeCP2 Affects Skeletal Muscle Growth and Morphology through Non Cell-Autonomous Mechanisms. *PLoS One*. 10:e0130183.

Cronk, J.C., N.C. Derecki, E. Ji, Y. Xu, A.E. Lampano, I. Smirnov, W. Baker, G.T. Norris, I. Marin, N. Coddington, Y. Wolf, S.D. Turner, A. Aderem, A.L. Klibanov, T.H. Harris, S. Jung, V. Litvak, and J. Kipnis. 2015. Methyl-CpG Binding Protein 2 Regulates Microglia and Macrophage Gene Expression in Response to Inflammatory Stimuli. *Immunity*. 42:679-91.

Damen, D., and R. Heumann. 2013. MeCP2 phosphorylation in the brain: from transcription to behavior. *Biol Chem*. 394:1595-605.

Dephoure, N., C. Zhou, J. Villen, S.A. Beausoleil, C.E. Bakalarski, S.J. Elledge, and S.P. Gygi. 2008. A quantitative atlas of mitotic phosphorylation. *Proc Natl Acad Sci U S A*. 105:10762-7.

Derecki, N.C., J.C. Cronk, Z. Lu, E. Xu, S.B. Abbott, P.G. Guyenet, and J. Kipnis. 2012. Wild-type microglia arrest pathology in a mouse model of Rett syndrome. *Nature*. 484:105-9.

Ebert, D.H., H.W. Gabel, N.D. Robinson, N.R. Kastan, L.S. Hu, S. Cohen, A.J. Navarro, M.J. Lyst, R. Ekiert, A.P. Bird, and M.E. Greenberg. 2013. Activity-dependent phosphorylation of MeCP2 threonine 308 regulates interaction with NCoR. *Nature*. 499:341-5.

Erlandson, A., and B. Hagberg. 2005. MECP2 abnormality phenotypes: clinicopathologic area with broad variability. *J Child Neurol*. 20:727-32.

Fischer, M., J. Reuter, F.J. Gerich, B. Hildebrandt, S. Hagele, D. Katschinski, and M. Muller. 2009. Enhanced hypoxia susceptibility in hippocampal slices from a mouse model of rett syndrome. *J Neurophysiol*. 101:1016-32.

Forlani, G., E. Giarda, U. Ala, F. Di Cunto, M. Salani, R. Tupler, C. Kilstrup-Nielsen, and N. Landsberger. 2010. The MeCP2/YY1 interaction regulates ANT1 expression at 4q35: novel hints for Rett syndrome pathogenesis. *Hum Mol Genet*. 19:3114-23.

Fuks, F., P.J. Hurd, D. Wolf, X. Nan, A.P. Bird, and T. Kouzarides. 2003. The methyl-CpG-binding protein MeCP2 links DNA methylation to histone methylation. *J Biol Chem*. 278:4035-40.

Georgel, P.T., R.A. Horowitz-Scherer, N. Adkins, C.L. Woodcock, P.A. Wade, and J.C. Hansen. 2003. Chromatin compaction by human MeCP2. Assembly of novel secondary chromatin structures in the absence of DNA methylation. *J Biol Chem*. 278:32181-8.

Ghosh, R.P., R.A. Horowitz-Scherer, T. Nikitina, L.S. Shlyakhtenko, and C.L. Woodcock. 2010a. MeCP2 binds cooperatively to its substrate and competes with histone H1 for chromatin binding sites. *Mol Cell Biol*. 30:4656-70.

Ghosh, R.P., T. Nikitina, R.A. Horowitz-Scherer, L.M. Gierasch, V.N. Uversky, K. Hite, J.C. Hansen, and C.L. Woodcock. 2010b. Unique physical properties and interactions of the domains of methylated DNA binding protein 2. *Biochemistry*. 49:4395-410.

Giacometti, E., S. Luikenhuis, C. Beard, and R. Jaenisch. 2007. Partial rescue of MeCP2 deficiency by postnatal activation of MeCP2. *Proc Natl Acad Sci U S A*. 104:1931-6.

Goffin, D., M. Allen, L. Zhang, M. Amorim, I.T. Wang, A.R. Reyes, A. Mercado-Berton, C. Ong, S. Cohen, L. Hu, J.A. Blendy, G.C. Carlson, S.J. Siegel, M.E. Greenberg, and Z. Zhou. 2012. Rett syndrome mutation MeCP2 T158A disrupts DNA binding, protein stability and ERP responses. *Nat Neurosci*. 15:274-83.

Gonzales, M.L., S. Adams, K.W. Dunaway, and J.M. LaSalle. 2012. Phosphorylation of distinct sites in MeCP2 modifies cofactor associations and the dynamics of transcriptional regulation. *Mol Cell Biol*. 32:2894-903.

Guy, J., H. Cheval, J. Selfridge, and A. Bird. 2011. The role of MeCP2 in the brain. *Annu Rev Cell Dev Biol*. 27:631-52.

Guy, J., J. Gan, J. Selfridge, S. Cobb, and A. Bird. 2007. Reversal of neurological defects in a mouse model of Rett syndrome. *Science*. 315:1143-7.

Guy, J., B. Hendrich, M. Holmes, J.E. Martin, and A. Bird. 2001. A mouse Mecp2-null mutation causes neurological symptoms that mimic Rett syndrome. *Nat Genet*. 27:322-6.

Hagberg, B., J. Aicardi, K. Dias, and O. Ramos. 1983. A progressive syndrome of autism, dementia, ataxia, and loss of purposeful hand use in girls: Rett's syndrome: report of 35 cases. *Ann Neurol*. 14:471-9.

Hansen, J.C., R.P. Ghosh, and C.L. Woodcock. 2010. Binding of the Rett syndrome protein, MeCP2, to methylated and unmethylated DNA and chromatin. *IUBMB Life*. 62:732-8.

Harikrishnan, K.N., M.Z. Chow, E.K. Baker, S. Pal, S. Bassal, D. Brasacchio, L. Wang, J.M. Craig, P.L. Jones, S. Sif, and A. El-Osta. 2005. Brahma links the SWI/SNF chromatin-remodeling complex with MeCP2-dependent transcriptional silencing. *Nat Genet*. 37:254-64.

Higginbotham, H.R., and J.G. Gleeson. 2007. The centrosome in neuronal development. *Trends Neurosci*. 30:276-83.

Inui, K., M. Akagi, J. Ono, H. Tsukamoto, K. Shimono, T. Mano, K. Imai, M. Yamada, T. Muramatsu, N. Sakai, and S. Okada. 2001. Mutational analysis of MECP2 in Japanese patients with atypical Rett syndrome. *Brain Dev*. 23:212-5.

Itoh, M., C.G. Tahimic, S. Ide, A. Otsuki, T. Sasaoka, S. Noguchi, M. Oshimura, Y. Goto, and A. Kurimasa. 2012. Methyl CpG-binding protein isoform MeCP2_e2 is dispensable for Rett syndrome phenotypes but essential for embryo viability and placenta development. *J Biol Chem*. 287:13859-67.

Jeffery, L., and S. Nakielny. 2004. Components of the DNA methylation system of chromatin control are RNA-binding proteins. *J Biol Chem*. 279:49479-87.

Jones, P.L., G.J. Veenstra, P.A. Wade, D. Vermaak, S.U. Kass, N. Landsberger, J. Strouboulis, and A.P. Wolffe. 1998. Methylated DNA and MeCP2 recruit histone deacetylase to repress transcription. *Nat Genet*. 19:187-91.

Kelleher, R.J., 3rd, and M.F. Bear. 2008. The autistic neuron: troubled translation? *Cell*. 135:401-6.

Kilstrup-Nielsen, C., L. Rusconi, P. La Montanara, D. Ciceri, A. Bergo, F. Bedogni, and N. Landsberger. 2012. What We Know and Would Like to Know about CDKL5 and Its Involvement in Epileptic Encephalopathy. *Neural Plast*. 2012:728267.

Kim, S., and B.D. Dynlacht. 2013. Assembling a primary cilium. *Curr Opin Cell Biol*. 25:506-11.

Kimura, H., and K. Shiota. 2003. Methyl-CpG-binding protein, MeCP2, is a target molecule for maintenance DNA methyltransferase, Dnmt1. *J Biol Chem*. 278:4806-12.

Kishi, N., and J.D. Macklis. 2004. MECP2 is progressively expressed in post-migratory neurons and is involved in neuronal maturation rather than cell fate decisions. *Mol Cell Neurosci*. 27:306-21.

Kokura, K., S.C. Kaul, R. Wadhwa, T. Nomura, M.M. Khan, T. Shinagawa, T. Yasukawa, C. Colmenares, and S. Ishii. 2001. The Ski protein family is required for MeCP2-mediated transcriptional repression. *J Biol Chem*. 276:34115-21.

Kriaucionis, S., and A. Bird. 2004. The major form of MeCP2 has a novel N-terminus generated by alternative splicing. *Nucleic Acids Res*. 32:1818-23.

Kron, M., C.J. Howell, I.T. Adams, M. Ransbottom, D. Christian, M. Ogier, and D.M. Katz. 2012. Brain activity mapping in Mecp2 mutant mice reveals functional deficits in forebrain circuits, including key nodes in the default mode network, that are reversed with ketamine treatment. *J Neurosci*. 32:13860-72.

Kudo, S., Y. Nomura, M. Segawa, N. Fujita, M. Nakao, C. Schanen, and M. Tamura. 2003. Heterogeneity in residual function of MeCP2 carrying missense mutations in the methyl CpG binding domain. *J Med Genet*. 40:487-93.

Lewis, J.D., R.R. Meehan, W.J. Henzel, I. Maurer-Fogy, P. Jeppesen, F. Klein, and A. Bird. 1992. Purification, sequence, and cellular localization of a novel chromosomal protein that binds to methylated DNA. *Cell*. 69:905-14.

Li, H., X. Zhong, K.F. Chau, E.C. Williams, and Q. Chang. 2011. Loss of activity-induced phosphorylation of MeCP2 enhances synaptogenesis, LTP and spatial memory. *Nat Neurosci*. 14:1001-8.

Lioy, D.T., S.K. Garg, C.E. Monaghan, J. Raber, K.D. Foust, B.K. Kaspar, P.G. Hirrlinger, F. Kirchhoff, J.M. Bissonnette, N. Ballas, and G. Mandel. 2011. A role for glia in the progression of Rett's syndrome. *Nature*. 475:497-500.

Lombardi, L.M., S.A. Baker, and H.Y. Zoghbi. 2015. MECP2 disorders: from the clinic to mice and back. *J Clin Invest*. 125:2914-23.

Long, S.W., J.Y. Ooi, P.M. Yau, and P.L. Jones. 2011. A brain-derived MeCP2 complex supports a role for MeCP2 in RNA processing. *Biosci Rep*. 31:333-43.

Luikenhuis, S., E. Giacometti, C.F. Beard, and R. Jaenisch. 2004. Expression of MeCP2 in postmitotic neurons rescues Rett syndrome in mice. *Proc Natl Acad Sci U S A*. 101:6033-8.

Lunyak, V.V., R. Burgess, G.G. Prefontaine, C. Nelson, S.H. Sze, J. Chenoweth, P. Schwartz, P.A. Pevzner, C. Glass, G. Mandel, and M.G. Rosenfeld. 2002. Corepressor-dependent silencing of chromosomal regions encoding neuronal genes. *Science*. 298:1747-52.

Lyst, M.J., R. Ekiert, D.H. Ebert, C. Merusi, J. Nowak, J. Selfridge, J. Guy, N.R. Kastan, N.D. Robinson, F. de Lima Alves, J. Rappsilber, M.E. Greenberg, and A. Bird. 2013. Rett syndrome mutations abolish the interaction of MeCP2 with the NCoR/SMRT co-repressor. *Nat Neurosci*. 16:898-902.

Matsumura, S., L.M. Persson, L. Wong, and A.C. Wilson. 2010. The latency-associated nuclear antigen interacts with MeCP2 and nucleosomes through separate domains. *J Virol*. 84:2318-30.

McGraw, C.M., R.C. Samaco, and H.Y. Zoghbi. 2011. Adult neural function requires MeCP2. *Science*. 333:186.

Mellen, M., P. Ayata, S. Dewell, S. Kriaucionis, and N. Heintz. 2012. MeCP2 binds to 5hmC enriched within active genes and accessible chromatin in the nervous system. *Cell*. 151:1417-30.

Muotri, A.R., M.C. Marchetto, N.G. Coufal, R. Oefner, G. Yeo, K. Nakashima, and F.H. Gage. 2010. L1 retrotransposition in neurons is modulated by MeCP2. *Nature*. 468:443-6.

Nan, X., J. Hou, A. Maclean, J. Nasir, M.J. Lafuente, X. Shu, S. Kriaucionis, and A. Bird. 2007. Interaction between chromatin proteins MECP2 and ATRX is disrupted by mutations that cause inherited mental retardation. *Proc Natl Acad Sci U S A*. 104:2709-14.

Nan, X., P. Tate, E. Li, and A. Bird. 1996. DNA methylation specifies chromosomal localization of MeCP2. *Mol Cell Biol*. 16:414-21.

Neul, J.L., W.E. Kaufmann, D.G. Glaze, J. Christodoulou, A.J. Clarke, N. Bahi-Buisson, H. Leonard, M.E. Bailey, N.C. Schanen, M. Zappella, A. Renieri, P. Huppke, and A.K. Percy. 2010. Rett syndrome: revised diagnostic criteria and nomenclature. *Ann Neurol*. 68:944-50.

Park, M.J., S. Aja, Q. Li, A.L. Degano, J. Penati, J. Zhuo, C.R. Roe, and G.V. Ronnett. 2014. Anaplerotic triheptanoin diet enhances mitochondrial substrate use to remodel the metabolome and improve lifespan, motor function, and sociability in MeCP2-null mice. *PLoS One*. 9:e109527.

Pelka, G.J., C.M. Watson, J. Christodoulou, and P.P. Tam. 2005. Distinct expression profiles of Mecp2 transcripts with different lengths of 3'UTR in the brain and visceral organs during mouse development. *Genomics*. 85:441-52.

Percy, A.K., and J.B. Lane. 2005. Rett syndrome: model of neurodevelopmental disorders. *J Child Neurol*. 20:718-21.

Ricceri, L., B. De Filippis, and G. Laviola. 2008. Mouse models of Rett syndrome: from behavioural phenotyping to preclinical evaluation of new therapeutic approaches. *Behav Pharmacol*. 19:501-17.

Ricciardi, S., E.M. Boggio, S. Grosso, G. Lonetti, G. Forlani, G. Stefanelli, E. Calcagno, N. Morello, N. Landsberger, S. Biffo, T. Pizzorusso, M. Giustetto, and V. Broccoli. 2011. Reduced AKT/mTOR signaling and protein synthesis dysregulation in a Rett syndrome animal model. *Hum Mol Genet*. 20:1182-96.

Samaco, R.C., C.M. McGraw, C.S. Ward, Y. Sun, J.L. Neul, and H.Y. Zoghbi. 2013. Female Mecp2(+/-) mice display robust behavioral deficits on two different genetic backgrounds providing a framework for pre-clinical studies. *Hum Mol Genet*. 22:96-109.

Samaco, R.C., and J.L. Neul. 2011. Complexities of Rett syndrome and MeCP2. *J Neurosci*. 31:7951-9.

Schanen, C., E.J. Houwink, N. Dorrani, J. Lane, R. Everett, A. Feng, R.M. Cantor, and A. Percy. 2004. Phenotypic manifestations of MECP2 mutations in classical and atypical Rett syndrome. *Am J Med Genet A*. 126A:129-40.

Shahbazian, M., J. Young, L. Yuva-Paylor, C. Spencer, B. Antalffy, J. Noebels, D. Armstrong, R. Paylor, and H. Zoghbi. 2002a. Mice with truncated MeCP2 recapitulate many Rett syndrome features and display hyperacetylation of histone H3. *Neuron*. 35:243-54.

Shahbazian, M.D., B. Antalffy, D.L. Armstrong, and H.Y. Zoghbi. 2002b. Insight into Rett syndrome: MeCP2 levels display tissue- and cell-specific differences and correlate with neuronal maturation. *Hum Mol Genet*. 11:115-24.

Skene, P.J., R.S. Illingworth, S. Webb, A.R. Kerr, K.D. James, D.J. Turner, R. Andrews, and A.P. Bird. 2010. Neuronal MeCP2 is expressed at near histone-octamer levels and globally alters the chromatin state. *Mol Cell*. 37:457-68.

Smeets, E.E., K. Pelc, and B. Dan. 2012. Rett Syndrome. *Mol Syndromol*. 2:113-127.

Suzuki, M., T. Yamada, F. Kihara-Negishi, T. Sakurai, and T. Oikawa. 2003. Direct association between PU.1 and MeCP2 that recruits mSin3A-HDAC complex for PU.1-mediated transcriptional repression. *Oncogene*. 22:8688-98.

Tao, J., K. Hu, Q. Chang, H. Wu, N.E. Sherman, K. Martinowich, R.J. Klose, C. Schanen, R. Jaenisch, W. Wang, and Y.E. Sun. 2009. Phosphorylation of MeCP2 at Serine 80 regulates its chromatin association and neurological function. *Proc Natl Acad Sci U S A*. 106:4882-7.

Wang, J., J.E. Wegener, T.W. Huang, S. Sripathy, H. De Jesus-Cortes, P. Xu, S. Tran, W. Knobbe, V. Leko, J. Britt, R. Starwalt, L. McDaniel, C.S. Ward, D. Parra, B. Newcomb, U. Lao, C. Nourigat, D.A. Flowers, S. Cullen, N.L. Jorstad, Y. Yang, L. Glaskova, S. Vigneau, J. Kozlitina, M.J. Yetman, J.L. Jankowsky, S.D. Reichardt, H.M. Reichardt, J. Gartner, M.S. Bartolomei, M. Fang, K. Loeb, C.D. Keene, I. Bernstein, M. Goodell, D.J. Brat, P. Huppke, J.L. Neul, A. Bedalov, and A.A. Pieper. 2015. Wild-type microglia do not reverse pathology in mouse models of Rett syndrome. *Nature*. 521:E1-4.

Young, J.I., E.P. Hong, J.C. Castle, J. Crespo-Barreto, A.B. Bowman, M.F. Rose, D. Kang, R. Richman, J.M. Johnson, S. Berget, and H.Y. Zoghbi. 2005. Regulation of RNA splicing by the methylation-dependent transcriptional repressor methyl-CpG binding protein 2. *Proc Natl Acad Sci U S A*. 102:17551-8.

Zhou, Z., E.J. Hong, S. Cohen, W.N. Zhao, H.Y. Ho, L. Schmidt, W.G. Chen, Y. Lin, E. Savner, E.C. Griffith, L. Hu, J.A. Steen, C.J. Weitz, and M.E. Greenberg. 2006. Brain-specific phosphorylation of MeCP2 regulates activity-dependent Bdnf transcription, dendritic growth, and spine maturation. *Neuron*. 52:255-69.

# 6. Produced Publications

Neuroscience and Biobehavioral Reviews 46 (2014) 187–201

Contents lists available at ScienceDirect

Neuroscience and Biobehavioral Reviews

journal homepage: www.elsevier.com/locate/neubiorev

Review

## Rett syndrome and the urge of novel approaches to study MeCP2 functions and mechanisms of action

Francesco Bedogni[a,b], Riccardo L. Rossi[c], Francesco Galli[a], Clementina Cobolli Gigli[a,b], Anna Gandaglia[a,b], Charlotte Kilstrup-Nielsen[b], Nicoletta Landsberger[a,b,*]

[a] San Raffaele Rett Research Center, Division of Neuroscience, San Raffaele Scientific Institute, Milan 20132, Italy
[b] Laboratory of Genetic and Epigenetic Control of Gene Expression, Department of Theoretical and Applied Sciences, Division of Biomedical Research, University of Insubria, Busto Arsizio 21052, Italy
[c] Fondazione Istituto Nazionale Genetica Molecolare, Milan 20122, Italy

ARTICLE INFO

*Article history:*
Received 17 July 2013
Received in revised form 25 October 2013
Accepted 21 January 2014
Available online 2 March 2014

*Keywords:*
Rett syndrome
MeCP2
Structure and function
Molecular genetics
Perturbation in gene expression
Pathway enrichment analysis

ABSTRACT

Rett syndrome (RTT) is a devastating genetic disorder that worldwide represents the most common genetic cause of severe intellectual disability in females. Most cases are caused by mutations in the X-linked *MECP2* gene. Several recent studies have demonstrated that RTT mimicking animal models do not develop an irreversible condition and phenotypic rescue is possible. However, no cure for RTT has been identified so far, and patients are only given symptomatic and supportive treatments. The development of clinical applications imposes a more comprehensive knowledge of MeCP2 functional role(s) and their relevance for RTT pathobiology. Herein, we thoroughly survey the knowledge about MeCP2 structure and functions, highlighting the necessity of identifying more functional domains and the value of molecular genetics. Given that, in our opinion, RTT ultimately is generated by perturbations in gene transcription and so far no genes/pathways have been consistently linked to a dysfunctional MeCP2, we have used higher-level bioinformatic analyses to identify commonly deregulated mechanisms in MeCP2-defective samples. In this review we present our results and discuss the possible value of the utilized approach.


**Contents**



* Corresponding author at: Laboratory of Genetic and Epigenetic Control of Gene Expression, Department of Theoretical and Applied Sciences, Division of Biomedical Research, University of Insubria, Busto Arsizio 21052, Italy. Tel.: +39 0331339406.
*E-mail address:* landsben@uninsubria.it (N. Landsberger).

http://dx.doi.org/10.1016/j.neubiorev.2014.01.011
0149-7634/

PLOS | ONE

RESEARCH ARTICLE

# MeCP2 Affects Skeletal Muscle Growth and Morphology through Non Cell-Autonomous Mechanisms

**Valentina Conti[1☯], Anna Gandaglia[2,3☯], Francesco Galli[2], Mario Tirone[4,5], Elisa Bellini[2], Lara Campana[5,6], Charlotte Kilstrup-Nielsen[7], Patrizia Rovere-Querini[5,6], Silvia Brunelli[4]*, Nicoletta Landsberger[2,8]***

**1** Division of Regenerative Medicine, Stem Cells and Gene Therapy, San Raffaele Scientific Institute, Milan, Italy, **2** San Raffaele Rett Research Unit, Division of Neuroscience, San Raffaele Scientific Insitute, Milan, Italy, **3** University of Insubria, PhD School in Neurobiology, Busto Arsizio, Italy, **4** Department of Health Sciences, University of Milano-Bicocca, Monza, Italy, **5** Division of Immunology, Transplantation and Infectious Diseases, San Raffaele Scientific Institute, Milan, Italy, **6** Vita-Salute San Raffaele University, School of Medicine, Milan, Italy, **7** Laboratory of Genetic and Epigenetic Control of Gene Expression, Division of Biomedical Research, Department of Theoretical and Applied Sciences, University of Insubria, Busto Arsizio, Italy, **8** Department of Medical Biotechnology and Translational Medicine, University of Milan, Segrate Italy

☯ These authors contributed equally to this work.
* Nicoletta.landsberger@unimi.it (NL); silvia.brunelli@unimib.it (SB)



OPEN ACCESS

**Citation:** Conti V, Gandaglia A, Galli F, Tirone M, Bellini E, Campana L, et al. (2015) MeCP2 Affects Skeletal Muscle Growth and Morphology through Non Cell-Autonomous Mechanisms. PLoS ONE 10(6): e0130183. doi:10.1371/journal.pone.0130183

**Editor:** Maurizio D'Esposito, Institute of Genetics and Biophysics, ITALY

**Received:** March 3, 2015

**Accepted:** May 18, 2015

**Published:** June 22, 2015



**Data Availability Statement:** All relevant data are within the paper and its Supporting Information files.

**Funding:** Funding for this work was provided by Ministero dell'Istruzione, Università e Ricerca (PRIN2010-2011) to SB. Additional funding was provided by proRETT ricerca to NL. The funders had no role in study design, data collection and analysis, decision to publish, or preparation of the manuscript.

**Competing Interests:** The authors have declared that no competing interests exist.

## Abstract

Rett syndrome (RTT) is an autism spectrum disorder mainly caused by mutations in the X-linked *MECP2* gene and affecting roughly 1 out of 10.000 born girls. Symptoms range in severity and include stereotypical movement, lack of spoken language, seizures, ataxia and severe intellectual disability. Notably, muscle tone is generally abnormal in RTT girls and women and the *Mecp2*-null mouse model constitutively reflects this disease feature. We hypothesized that MeCP2 in muscle might physiologically contribute to its development and/or homeostasis, and conversely its defects in RTT might alter the tissue integrity or function. We show here that a disorganized architecture, with hypotrophic fibres and tissue fibrosis, characterizes skeletal muscles retrieved from *Mecp2*-null mice. Alterations of the IGF-1/Akt/mTOR pathway accompany the muscle phenotype. A conditional mouse model selectively depleted of *Mecp2* in skeletal muscles is characterized by healthy muscles that are morphologically and molecularly indistinguishable from those of wild-type mice raising the possibility that hypotonia in RTT is mainly, if not exclusively, mediated by non-cell autonomous effects. Our results suggest that defects in paracrine/endocrine signaling and, in particular, in the GH/IGF axis appear as the major cause of the observed muscular defects. Remarkably, this is the first study describing the selective deletion of *Mecp2* outside the brain. Similar future studies will permit to unambiguously define the direct impact of MeCP2 on tissue dysfunctions.

PLOS ONE

# MeCP2 related studies benefit from the use of CD1 as genetic background

--Manuscript Draft--

| | |
|---|---|
| **Manuscript Number:** | PONE-D-15-25567 |
| **Article Type:** | Research Article |
| **Full Title:** | MeCP2 related studies benefit from the use of CD1 as genetic background |
| **Short Title:** | CD1 background facilitates MeCP2 related studies |
| **Corresponding Author:** | Nicoletta Landsberger<br>Ospedale San Raffaele<br>Milan, ITALY |
| **Keywords:** | MeCP2, mouse models, genetic background, Rett syndrome. |
| **Abstract:** | MECP2 mutations cause a broad spectrum of neurological disorders of which Rett syndrome (RTT) represents the best-defined condition. Several mouse models of RTT have been generated whose face validity is demonstrated by the presence of a broad spectrum of phenotypes largely mimicking those manifested by RTT patients. Importantly, these models have permitted to demonstrate that RTT is not an irreversible condition. Although much has been produced describing the different roles played by Mepc2, still much is needed to possibly propose translational studies. Mouse models are therefore crucial for the identification of valid therapeutic approaches. Since most MECP2 pathogenic lesions are considered loss of function mutations, the Mecp2-null alleles have construct validity; accordingly, the C57/B6 Mecp2tm1.1Bird line probably represents the mostly used Mecp2 model. However, small litters with little viability, under-representation of the mutant allele and poor maternal care hamper colony maintenance, and severely limit research. To ameliorate and facilitate managing the Mecp2 null colony, we have transferred the Mecp2tm1.1Bird allele on the stronger and easier-to-breed CD1 background. The obtained strain recapitulates several phenotypes described in mouse models of Mecp2, but does not present the breeding difficulties encountered with the C57/B6 strain. The validity of this strain is strengthened by longer lifespan and better general conditions of the null animals. Thus, we believe that the use of this validated mouse model has the potentiality to improve research on RTT. |
| **Order of Authors:** | Clementina Cobolli Gigli |
| | Linda Scaramuzza |
| | Anna Gandaglia |
| | Elisa Bellini |
| | Charlotte Kilstrup Nielsen |
| | Nicoletta Landsberger |
| | Francesco Bedogni |
| **Opposed Reviewers:** | Elizabeth Fisher<br>Institute of Neurology, Queen Square London<br><br>Bias opinions in outbred backgrounds |
| | Michael Festing<br>University of Leicester<br><br>Bias opinions on outbred genetic backgrounds |
| **Additional Information:** | |
| **Question** | **Response** |
| **Financial Disclosure** | Jerome Lejeune Foundation to Francesco Bedogni<br>Jerome Lejeune Foundation to Nicoletta Landsberger<br>proRETT Ricerca to Nicoletta Landsberger |

# Ringraziamenti

Desidero ringraziare la Professoressa Daniela Parolaro, per la gentile supervisione durante questi tre anni di Dottorato.

Ringrazio sentitamente la Professoressa Nicoletta Landsberger, per avermi consentito di continuare il mio percorso formativo nel suo laboratorio, spronandomi a diventare una ricercatrice sempre più attenta ed indipendente, tuttavia senza mai privarmi della sua preziosa guida. La ringrazio per aver costantemente seguito l'andamento del mio Dottorato e dei progetti affidatimi, per tutti i suoi insegnamenti e – non da ultimo – per il tempo che mi ha dedicato. La ringrazio per la passione verso la ricerca scientifica che continuamente dimostra e trasmette.

Ringrazio l'Associazione ProRett, per essere stata grande fonte di motivazione e perché senza il suo aiuto economico questo Dottorato e questo progetto non sarebbero stati possibili.

Desidero ringraziare tutti i membri del San Raffaele Rett Research Center: Francesco, Angelisa, Gilda, Clementina, Linda, Chiara ed Elena. Ognuno di loro è parte fondamentale delle mie giornate lavorative, donandomi preziosi aiuti e consigli, nonché amicizia ed allegria. Un pensiero particolare va a Chiara, la cui collaborazione è stata indispensabile per lo svolgimento di questo progetto, e a Clementina, per tutti questi anni condivisi fianco a fianco. Desidero inoltre ringraziare Anna e Barbara del laboratorio di Busto Arsizio, per l'importante scambio di idee e di dati.

Ringrazio tutte le amiche e tutti gli amici che con il loro affetto e la loro simpatia mi hanno accompagnato durante questi anni di crescita personale. Un enorme grazie alla Sofy e all'Ale.

Ringrazio Ste, per avermi continuamente sostenuta, sopportata e spronata. Per credere in me.

Ringrazio tutta la mia famiglia, per la forza che mi da, per i sacrifici fatti per me, per essermi accanto in ogni momento.